HIGH VELOCITY IMPACTS

by

ARFON HARRY JONES

B. Sc. (Hons.), University of Leeds, 1955.

SUBMITTED IN PARTIAL FULFILLMENT OF THE
REQUIREMENTS FOR THE DEGREE OF
MASTER OF SCIENCE
at the
MASSACHUSETTS INSTITUTE OF TECHNOLOGY
1960

Signature of Author Signature redacted
Department of Aeronautics and Astronautics
January, 1960

Certified by Signature redacted
Thesis Supervisor

Signature redacted
Chairman, Departmental Committee of Graduate Students

Signature redacted

HIGH VELOCITY IMPACTS

by

Arfon Harry Jones

Submitted to the Department of Aeronautics and Astronautics on January 18, 1960, in partial fulfillment of the requirements for the degree of Master of Science.

ABSTRACT

The theory of high speed spherical flow in incompressible materials is presented for a pressure applied at the center of the sphere. This theory is used to estimate the radius of the zone of plastic deformation in a semi-infinite block due to impact by a small, high velocity, projectile, which is assumed to penetrate the target in the manner predicted by an hydrodynamic theory, assuming steady state.

The theoretical predictions are compared with the measured values obtained for targets of 70:30 brass, and 1/8 in diameter hardened steel projectiles.

Thesis Supervisor: R. L. Bisplinghoff

Title: Professor of Aeronautics and Astronautics.

January 18, 1960

Professor Philip Franklin
Secretary of the Faculty
Massachusetts Institute of Technology
Cambridge 39, Massachusetts

Dear Professor:

In accordance with the regulations of the faculty, I hereby submit a thesis entitled High Velocity Impacts in partial fulfillment of the requirement for the degree of Master of Science in Aeronautical Engineering.

Sincerely,

Arfon H. Jones

ACKNOWLEDGMENT

The author wishes to express his thanks to Professor R. L. Bisplinghoff, who, as thesis supervisor, inspired the work, and to he and Dr. W. Herrmann, Research Engineer, Aeroelastic and Structural Laboratory, for their valuable help and criticism. The experimental work was embarked upon after discussions with Professor J. Wulff, Metallurgy Department, to whom the author is indebted; also to Professor D. A. Thomas and S. Oliver for their valuable discussions on the experimental techniques and their help in obtaining the 70:30 brass target.

Last, but by no means least, the author wishes to express his grateful thanks and appreciation to the English Speaking Union of the United States for awarding him a King George VI Memorial Scholarship. This award enabled the author to study at the Massachusetts Institute of Technology.

TABLE OF CONTENTS

CHAPTER 1

SUMMARY OF PREVIOUS WORK

High velocity impact may be considered in two parts (a) impact, penetration of the target material, and forces involved in impact, and (b) the stress waves set up by the impact.

1.1 Impact

In recent years a large number of papers have been published on the mechanism of cratering and penetration of targets by high velocity particles (see bibliography of ref. 1). Theories for penetration and volume of crater produced have been put forward by many of the authors. These have either been empirical, based on dimensional analysis, or simple hydrodynamic theory.

Projectiles suffer severe inelastic deformation on striking their target. Metal missiles may flow plastically, melt, vaporise, or shatter; for instance impact at very high velocity, usually above 4,000 ft/sec may generate enough heat to vaporize a steel projectile. The kinetic energy of the projectile appears to be finally distributed in

(a) work of deformation and structural changes of both the target and the projectile material.

(b) work of fracturing of both materials.

(c) kinetic energy of the target and projectile matter thrown out of crater (or off the target),

(d) energy for melting and vaporizing portions of both material, and

(e) heating of the material.

The shape and size of the crater produced will depend upon the shape, mass, and velocity of the projectile and upon the mechanical properties of the target. Cratering in steel usually results from plastic flow of the steel. At low velocities, below about 4,000 ft/sec, the crater is simply a straight-sided hole whose cross-section is similar to that of the impacting missile. At highest velocities, cavitation sets in and the profile of the hole is more or less circular and the diameter of the mouth considerably greater than that of the impacting missile. At very high velocities, greater than about 10,000 ft/sec, the crater will have a cup shaped appearance.

Cook [(2)*] has observed that a nearly hemispherical crater is produced when a single particle projectile of spherical form strikes a target at velocity sufficiently high that $\frac{1}{2} \rho_p (V - U)^2$ is appreciably greater than the yield strength of the target Y, where ρ_p is the density of the projectile, V its velocity, and U the steady

\- - - - - - - - - - - - - - - - -

*The figures appearing in superscript pertain to the references appended to the thesis.

velocity of penetration. Then the target undergoes plastic flow until the yield force $A'Y$ balances the dynamic force $\frac{1}{2}\rho_p(V-U)^2A_o$ where A' is the cross-sectional area of the hole at depth of penetration, and A_o the cross-sectional area of the projectile. Where single particles of nearly spherical shape are involved, this plastic flow is always radial except for conditions right at the surface of the target where an elevated lip is always observed owing to some back flow caused by relief of pressure at the surface.

The reason for the use of the hydrodynamic theory is that the pressure produced by the projectile at these high velocities are so much greater than the ultimate strength of the target, that its strength plays a negligible role in retarding the penetration, hence the target may be considered as a perfect fluid. The depth of penetration is given by Cook[2], Pack and Evans[3], and Birkhoff, MacDougall, Pugh and Taylor[4], assuming steady state conditions, in the form

$$\delta = d_p\left(\lambda\rho_p/\rho_t\right)^{1/2} \qquad 1$$

where d_p is the diameter of the projectile, λ a number between 1 (for a continuous jet) and 2(for a particulate jet), and ρ_t the density of the target. As pointed out this equation is considered to hold for a target neglecting the effect of yield strength. Pack and Evans[3] have modified the steady state theory to take into account the finite yield strength, by introducing the factor $\left(1 - \alpha_1 \frac{Y}{\rho_p V^2}\right)$ into the above equation where Y is the dynamic yield strength of the target and α_1 a constant which is a function of the densities of the particle and the target.

Cook[2] gives the final hole diameter as

$$D = d_p \frac{\cdot V(\rho_p \rho_t \lambda)^{1/2}}{[\rho_t^{1/2} + (\lambda \rho_p)^{1/2}]} \frac{1}{(2Y)^{1/2}} \qquad 2$$

where Y is the dynamic strength of the target. The hole volume for $\lambda = 1$ is

$$\tau = \frac{\rho_p^{1/2} \rho_t^{1/2}}{[\rho_p^{1/2} + \rho_t^{1/2}]^2} \cdot \left(\frac{3 m_p V^2}{4 Y} \right) \qquad 3$$

Engel[5] obtained an expression for the depth of penetration

$$\delta = \frac{7 \cdot 2}{1 + \frac{c_t \rho_t}{c_p \rho_p}} \left(\frac{V}{C_p} \right) - \frac{136 \cdot 8 \, E_t \rho_p^{1/2}}{\rho_t^{3/2} \, c_t^2} \qquad 4$$

This equation is derived from dimensional analysis, experimental results, and analysis.

Huth[6] found the empirical equation

$$\delta = 7 \cdot 95 \left(\frac{V}{c_t} \right)^{1 \cdot 4} \qquad 5$$

while Vellenburg, Clay and Huth[6] found from semi-empirical method

$$\delta = 6 \cdot 95 \left(\frac{\rho_p}{\rho_t} \right)^{1/3} \frac{V/c}{(3 - 1 \cdot 66 V/c_t)^{1/3}} \qquad 6$$

Partridge and Clay[7], from empirical work, obtained the expression

$$\delta = K M^{1/3} (V - U)/c_t \qquad 7$$

Where M is the mass of the projectile. Helie[9] and, Wessman and Rose[8], found on assuming the resistance to penetration to be the sum of two terms, a constant and a velocity squared term, that

$$\delta = K_1 \frac{M}{A} \log_e (1 + K_2 V^2)$$

where K_1 and K_2 are constants which depend upon such factors as the shape of the projectile, the density of the target material, and its resistance to penetration.

Rinehart[1] suggested that the size and shape of the crater (in extremely high velocity impact) depend primarily upon the stress distribution existing in the target during and immediately following deceleration of the missle. Stresses greatly in excess of those required to cause common materials to fail will exist during penetration in thos regions near the area of impact. Penetration depth and crater shape are arrived at by assuming (a) that the missile is stopped in a negligibly short distance, (b) that the forces of the impact distributes itself within the target in accordance with the same geometry as the stresses produced by a static load, and (c) that the target material will fail within a region in which the shearing stress exceeds a certain critical value.

1.2 Stress Waves

Stress Waves are divided into three types, two of these namely the elastic and plastic waves depend on the stress level, and the third type depend on the additional stresses. The stresses in the elastic waves are such that they obey Hooke's laws, while those plastic waves occur in material which undergoes permanent deformation as a result of being stressed beyond the elastic limit. Viscous waves occur when the internal viscous stresses are produced in addition to the other stresses, i.e. elastic or plastic. The viscous stresses are fairly small for metals, but are appreciable for materials that show large time effects in their behaviors under stresses.

For elastic waves a large amount of both theoretical and experimental work has been done. A review of these may be read in Kolsky[10], Davies[11], and Abramson, Plass and Ripperger[12] for bars and beams.

There is little published experimental work on wave propogation in non-linear visco-elastic solids. The work done in this field has been recently reviewed by Kolsky[13].

Plastic waves occur in material for low velocity of impact. For instance if we consider the impact of a rigid body on an elastic rod, the velocity that will produce plastic waves is given by

$$V = \frac{Yc}{E} \qquad 8$$

Where Y is the yield stress of the material, C the velocity of propogation of longitudinal waves in the material, and E Young's modulus. For aluminum we have

$E = 10^7$ p.s.i; $Y = 50,000$ p.s.i.; $C = 20,000$ ft/sec

which gives $V = 100$ ft/sec, and in the case of steel $E = 30 \times 10^6$ p.s.i; $Y = 45,000$ p.s.i and $c = 19,500$ ft/sec, hence $V = 30$ ft/sec.

The general one dimensional problem of the propogation of plastic waves was investigated independently by Taylor[14], von Karman[15] and Rakmatoolin[16]. Taylor [14] obtained the expression for propogation (using Eulerian system of coordinates)

$$c^2 = \frac{(1+\varepsilon)^2}{\rho_0} \frac{d\sigma}{d\varepsilon} \qquad 9$$

where ε is the strain

σ the stress corresponding to ε,

ρ_0 the density of the material.

and c the velocity of propogation.

Karman [15] obtained the corresponding expression in terms of Lagrangian system

$$c^2 = \frac{1}{\rho_0} \frac{d\sigma}{d\varepsilon} \qquad 10$$

Wood[17] has discussed the propogation of longitudinal waves of large lateral extend in solids for the elastic plastic condition. The stress-strain relation (assumed to be independent of time) is derived indirectly from experimental data by means of a suitable theory of plasticity, assuming the material is uncompressible. A specific example is worked for 24 S-T alūminum alloy,

$$E = 10.6 \times 10^6 \text{ p.s.i} , \quad \nu = 0.33$$

The velocity of the elastic and plastic waves are 2.46×10^5 in/sec and 2.01×10^5 in/sec. In a slender wire the corresponding plastic wave would have been of the order of 2.5×10^4 in/sec. This illustrates that lateral inertia may not be neglected.

Craggs[18] showed that for an elastic-plastic material, plane waves of two types may exist, each involving both dilatational and shear strain. However, the waves studied in Craggs' work have infinitesimal discontinuities in stress and strain existing across the wave front.

Thomas[19] investigated the propogation of plane plastic waves by considering the wave front as a singular surface of order one. Using various conditions, e.g. (i) von Mises theory for perfect plastic solids and only derivatives of velocity and stress as discontinuities, (ii) Prandtl-Reuss theory with discontinuities in derivatives of velocity and stress, and $\sigma'_1 \nu_2^2 + \sigma'_2 \nu_1^2 = 0$ over the wave surface, where σ'_1, σ'_2 are the deviator stress and ν_1, ν_2 the components of the unit normal vector to the surface, he obtains expressions for the velocity of the wave front. In the case of the above conditions, the velocity of propogation were (I) C = O, and (II) either

$$\left\{\mu + \tfrac{1}{2}\sigma'_1/\rho\right\}^{1/2} \quad \text{or} \quad \left\{\mu + \tfrac{1}{2}\sigma'_2/\rho\right\}^{1/2}$$

Berg[20] extended this for elastic-plastic work hardening materials. He found that both dilatation and equivoluminal waves could propogate in the medium, and that the velocity of each of these waves is a function of the state of plastic strain of an element on the wave and of the state of stress on the wave.

Experimental results indicate that there is a strain-rate effect which should be considered in the propogation of plastic waves. In most cases it is found that an increase in the rate of deformation will raise (a) the yield stress of the material (b) the entire stress level of the flow curve, and (c) the ultimate strength of the material. Taylor[21] found that for mild steel that the dynamic yield stress was about 3 times the static for impact strain of 10, 000 in/in/sec; also that the dynamic is nearly the same as the static yield point when steel with a high static yield is used.

Malvern[23] modified the one-dimensional theory of plastic wave propogation to introduce the effect of rate of strain on the stress-strain relation. He assumes a stress-strain relation of the form

$$E_0 \dot{\varepsilon}_x = \dot{\sigma}_x \qquad \text{elastic}$$

$$E_0 \dot{\varepsilon}_x = \dot{\sigma}_x + g(\sigma_x, \varepsilon_x) \qquad \text{plastic.}$$

and plastic flow occurs when $\sigma_x > f(\varepsilon_x)$. In order to approximate for hardened alumiuum specimens Malvern assumed

$$g(\sigma_x, \varepsilon_x) = k[\sigma_x - f(\varepsilon_x)]$$

and

$$f(\varepsilon_x) = 20,000 - \frac{10}{\varepsilon_x}$$

Comparing theory and practic he concluded that the theory gave better agreement than the predictions of elementary theory, but the permanent strain distribution was in worse agreement.

CHAPTER 2

MATHEMATICAL FORMULATION

In the mathematical theory of the mechanics of continuous media, the expression for large strain in direction one (1) is

$$E_1 = \sqrt{\frac{G_{11}}{g_{11}}} - 1 \qquad 11$$

where G_{11} and g_{11} are the metric tensors for the deformed and undeformed body respectively, in terms of the coordinate system in the original body. For finite strain this is approximated to

$$e_{11} = \frac{1}{2}\left(\frac{G_{11}}{g_{11}} - 1\right) \qquad 12$$

Except for the simplest cases (Zerna and Green)[42] the equations resulting from the approximation are unmanageable.

The linear (classical) theory of elasticity assumes infinitesimal strains. Here the strain-displacement relations* by neglecting products of derivatives of the displacement as compared with linear terms. For example in an arbitrary orthogonal coordinate system, if ε and ϖ are the infinitesimal strains and rotations,

*are an approximation obtained from the finite strain expression the finite strain is given by

$$e_{11} = \varepsilon_{11} + \frac{1}{2}\left[\varepsilon_{11}^2 + \left(\frac{1}{2}\varepsilon_{12} + \omega_{12}\right)^2 + \left(\frac{1}{2}\varepsilon_{13} - \omega_{13}\right)^2\right] \tag{13}$$

In applying the infinitesimal strain approximation to our problem we preclude any quantitative comparison with the results obtained in practice for a volume in the region of the crater. However, St. Venant's Principle leads us to believe that further away we should expect a good comparison.

In some experimental work carried out by Allen(30), it was pointed out that there was a similarity between the magnitude of the stresses measured in a steel plate due to a localized explosive load and an equivalent theoretical elastic calculation for a sphere assuming the application of pressure in a spherical cavity at the center. We carry out a similar analysis here for various theories since at very high pressure, we can neglect shear in both the elastic - plastic theory and the hydrodynamic theory (medium strength is assumed to be zero), taking an impulsive pressure p_0 acting for a time t', the penetration time, in a cavity of radius 'a' at the center of an infinite sphere.

The essential difference is that in the sphere we have spherical symmetry which precludes shear waves consideration, and the problem reduces to one dimension. Axial symmetric conditions require that shear in the Rz plane should be taken into account.

2.1 Hydrodynamical Theory.

The pressure produced by collision is given by

$$p_o = \frac{1}{2} \rho_t U^2 \qquad 14$$

The ultimate yield stress of cartridge-brass is on the order of 16,000 lb/in^2 (o. ooll megabars). All of the pressures encountered in impacts above 3,500 ft/sec are over 10 times in excess of the yield. Since this pressure is far above the material's yield strength, the strength may be neglected for a first approximation.

The equations of motion for the process, neglecting the viscosity and heat conduction, are the compressible, inviscid, adiabatic hydrodynamic. When the wave reaches the layer at a distance r from the origin, then, in the Lagrangian method, we follow the subsequent history of this layer. Let us suppose that at a time t is has radius R . Then r and t are the Lagrangian independent variables and the equations of motion are

$$\frac{\rho_o}{\rho} = \frac{R^2}{r^2}\left(\frac{\partial R}{\partial r}\right) \qquad 15$$

$$\frac{\partial^2 R}{\partial t^2} = -\frac{1}{\rho}\left(\frac{\partial p}{\partial R}\right) \qquad 16$$

$$S_t = 0 \qquad 17$$

$$p = f(\rho, S) \quad \text{--equation of state} \qquad 18$$

2.2 Solid Media

In obtaining the equation of motion for a solid media, we will assume infinitesimal strain. The equation of equilibrium is

$$\rho \frac{D^2 u_R}{Dt^2} = \frac{1}{R^2}\frac{\partial}{\partial R}\left(R^2 \sigma_R\right) - \frac{1}{R}\left(\sigma_\theta - \sigma_\varphi\right) \qquad 19$$

where D indicates the total derivative, and ρ is the density of the deformed media.

The strain-displacement relation for the medium will be

$$\varepsilon_R = \frac{\partial u_R}{\partial R} \;, \quad \varepsilon_\theta = \frac{u_R}{R} \;, \quad \varepsilon_\varphi = \frac{u_R}{R} \qquad 20$$

The continuity equation is

$$\frac{\partial \rho}{\partial t} + \frac{1}{R^2}\frac{\partial}{\partial R}\left(R^2 \rho\, \dot{u}_R\right) = 0 \qquad 21$$

where $\dot{u}_R = \frac{\partial u_R}{\partial t}$ 22

If we consider the incompressible solution then the above equation reduced to

$$\frac{1}{R^2}\frac{\partial}{\partial R}\left(R^2 \dot{u}_R\right) = 0$$

which may be written

$$\frac{1}{R^2}\frac{\partial}{\partial R}\left(R^2 u_R\right) = 0 \qquad 23$$

i.e.

$$\varepsilon_R + \varepsilon_\theta + \varepsilon_\varphi = 0 \qquad 24$$

2.3 Equations of State and the Stress-Strain Relations.

The equation of state is the relation between the properties of the material which uniquely describes the behaviour of the particular material in terms of only two independent properties, all other properties being functions of these two independent properties. For this equation to apply the material must remain in equilibrium. Furthermore, if phase changes occur a more complex equation of state will be required. Under explosive loading non-equilibrium conditions and phase changes do occur; however, in order not to further complicate the problem, we will neglect these here.

The experimental work required preliminary to obtaining the equation of state for metals has been carried out in two ways (I) static tests, and (II) shock propogation. Static tests (Bridgman)[24] gave us the isothermal equation of state, while the shock propogation method gave the Hugoniot. It is possible to calculate both the adiabats and isothermal from the theomodynamics and quantum mechanics consideration using the Hugoniot data as the initial condition.

The calculated offsets between the Hugoniot curve and the neighboring P--V curves of interest are generally small [Walsh, et al, 1957][26] to within 4% in compression for pressures below 200 kbs, for most metals [Katz et al, 1959][27]. Furthermore, Walsh et al, 1957, found that the Hugoniot curves which are drawn through the experimental points are reproduced by analytical fits of the form

$$p = A\mu + B\mu^2 + C\mu^3 \qquad 25$$

where

$$\mu = \frac{\rho}{\rho_0} - 1 \qquad 26$$

Values of A, B, and C for various solieds are listed[26], for example, 60:40 brass, this equation gives the pressure in kilobars for A=1037, B=2177, C=3275. Due to the small offset of the adiabat from the Hugoniot the error resulting in assuming the adiabat equation to be that of the Hugoniot would be small for pressures below 200 kbs.

Using the steady°state condition expression for the impact pressure, we find that for the present problem the pressures at impact would be less than 46 kilobars. This means that μ would be less than .04, hence a good approximation may be obtained by assuming incompressibility.

The elastic theory for the propogation of waves in the elastic media is based on the assumption that Hooke's law is valid, i.e. the equation of state is of the form $\sigma = E\,\varsigma(\varepsilon)$, in other words the stress at a given point in the medium at time t is proportional to the strain ε. At high strain rate, non-Hookean stresses have to be considered especially in the case of non-metallic alloys. In this respect analyses have been carried out on the propogation of stress waves for Kelvin-Voigt, Maxwell, and standard linear solid by Eubanks[35], Lee and Kanter[36], Hillier[37], etc. The true picture of deformation following impact would be given by the analysis of the motion of dislocations.

When a high stress is applied to a crystalline solid, it acquires elastic strain almost immediately. But in order to undertake permanent strains, dislocations must first be accelerated and multiplied. Dislocations comprising the Frank-Read sources accelerate rapidly because of their small effective mass; however, their inherent inertia should result in zero initial strain rate, followed as the dislocations form and accelerate by an increasing strain rate. The back stresses produced by the interaction of dislocations causes the strain rate to decrease, until finally, it becomes zero.

The stress-strain relation formulated from the consideration of the dynamics of dislocation will be a function of the strain rate, the instantaneous magnitudes of σ and ε, and the distribution of dislocations in the material at that time. The distribution of dislocations will depend on the stress history of the material and this is not exactly described by the state of strain alone.

Suitable movement of partial dislocations can produce the shear displacements which occur in mechanical twinning and in some phase transformations. Frank (1952, private communication with Narbarro) has discussed the martensitic transformation from face centered to body centered iron.

Up to the present, dislocation theory has not yet been sufficiently highly developed to permit derivation of the stress-strain equation from fundamental principles. In the following analysis we will neglect time dependent effects on the stress-strain relation.

In the present analysis we will consider the following stress-strain relations--

(I) Elastic

$$\left.\begin{aligned}\sigma_R &= 3\lambda e + 2G\varepsilon_R\\ \sigma_\theta &= 3\lambda e + 2G\varepsilon_\theta\\ \sigma_\varphi &= 3\lambda e + 2G\varepsilon_\varphi\end{aligned}\right\} \qquad 27$$

where

$$\lambda = \frac{\nu E}{(1+\nu)(1-2\nu)} \qquad \text{and} \qquad e = \frac{1}{3}(\varepsilon_R + \varepsilon_\theta + \varepsilon_\varphi)$$

(II) Plastic

The Levy-Mises relation for the stress-strain increment in a plastic media may be expressed in the form

$$\frac{d\varepsilon_R}{\sigma_R^*} = \frac{d\varepsilon_\theta}{\sigma_\theta^*} = \frac{d\varepsilon_\varphi}{\sigma_\varphi^*} = \frac{d\Omega}{2G} \qquad 28$$

where $\sigma_R^* = \frac{1}{3}(2\sigma_R - \sigma_\theta - \sigma_\varphi) = \sigma_R - \sigma$

and $d\Omega$ is a scalar factor of proportionality. Since these equations assume the total strain increment, and not the plastic strain increment these equations are strictly applicable only to a fictitious material in which the elastic strains are zero. In this case Young's modulus is indefinitely large, the material remaining rigid when unloaded.

Reuss extended these equations in order to allow for the elastic component of strain. He assumed

$$\frac{d\varepsilon_R^p}{\sigma_R^*} = \frac{d\varepsilon_\theta^p}{\sigma_\theta^*} = \frac{d\varepsilon_\varphi^p}{\sigma_\varphi^*} = \frac{d\Omega}{2G} \qquad 29$$

where ϵ_{ij}^{p} is the plastic component of strain. Neither these nor the Levy-Mises set of stress-strain relations reflect any viscosity effect.

Since we have introduced a further variable we need one more equation, this is provided by the yield condition.

$$f(\sigma) = Y$$

where Y is the yield stress in simple tension.

2.4 Yield Condition

Plastic deformation of crystalline materials is known to arise from the motion of dislocations. In the unyielded condition, the dislocations are anchored and the deformation is purely elastic, while in the overstrained condition the dislocations are free to move under the applied stress and so produce plastic deformations. The yield defines the limit of elasticity under any possible combination of stress.

Experimental work has shown that the yielding of a metal is unaffected by hydrostatic pressure or tension either applied alone or superposed, but varies with the rate of straining. Taylor[21] has obtained results showing that the yielding of mild steel at the rate of straining of 10,000 in/in/sec occurs in the order of three times the static yield stress. The dynamic yield is nearly the same as the static yield when steel with a high static yield is used. This ratio tends to rise as the static yield decreases. In the following analysis we will neglect this effect on the yield stress.

The two simplest yield criteria which does not conflict with the static observation are those of Tresca and von Mises. Tresca stipulates that during plastic flow the greatest of the principal shearing stresses has a constant value,

$$\sigma_{I} - \sigma_{III} = Y \qquad 30$$

where $\sigma_{I} \geq \sigma_{II} \geq \sigma_{III}$ and $\sigma_{I}, \sigma_{II}, \sigma_{III}$ are the principal stress. Von Mises criterion is

$$(\sigma_{I} - \sigma_{III})^2 + (\sigma_{II} - \sigma_{III})^2 + (\sigma_{III} - \sigma_{I})^2 = 2Y^2. \qquad 31$$

For the spherically symmetrical problem, both the Tresca and von Mises condition reduce to

$$\sigma_{\theta} - \sigma_{R} = Y \qquad 32$$

for $d\varsigma \geq 0$

where $d\varsigma > 0$ implies compressive loading.

2.5 Initial and Boundary Conditions.

The pressure at the cavity is assumed to be that presented on the target by the projectile. This is expressible in the form

$$p_0 = 0 \qquad 0 \geq t$$

$$p_0 = \frac{1}{2} \frac{\lambda \rho_p \rho_t}{\left[(\rho_t)^{1/2} + (\lambda \rho_p)^{1/2} \right]^2} V^2 \qquad 0 \leq t < t' \qquad 33$$

where t' is the time for penetration.

$$t' = \frac{d}{V}\left\{ 1 + \left(\frac{\lambda \rho_p}{\rho_t} \right)^{1/2} \right\} \tag{34}$$

These expressions are based on the steady state hydrodynamical theory.

The boundary conditions are at $R = a$, the current radius of the cavity

$$(\sigma_R)_a = 0 \qquad\qquad 0 \geq t$$

$$(\sigma_R)_a + p(t) = 0 \qquad\qquad 0 \leq t \leq t' \tag{35}$$

and, as $R \to \infty$, we have

$$\underset{R \to \infty}{Lt} (\sigma_R) \to 0 \quad \text{and} \quad \underset{R \to \infty}{Lt} (\sigma_\theta) \to 0 \tag{36}$$

For the plastic problem we have a further condition at $R = c(t)$ i.e. the moving boundary $\sigma_\theta - \sigma_R = Y$; this is the Rankine-Hugoniot quantity

$$\sigma_R - \rho \dot{u}_R (\dot{u}_R - \dot{c}) = \text{const.} \tag{37}$$

2.6 Theory of Incompressible Flow.

The spherically symmetric flow is described in terms of a position vector R, which indicates the position of a spherical shell initially located at r. Clearly

$$R(r,t) = r + u(r,t) \tag{38}$$

defining the displacement $u(r,t)$. In assuming incompressibility we impose the following conditions

$$\frac{R^2}{r^2}\frac{\partial R}{\partial r} = 1 \tag{15}$$

$$\left.\begin{aligned} \rho &= \rho_0 \\ \nu &= 1/2 \\ e &= 0 \end{aligned}\right\} \tag{39}$$

On integrating the above equation we obtain

$$R^3 = r^3 + 3\xi(t) \tag{40}$$

where $\xi(t)$ is a function of time to be determined. In order to satisfy the initial state $t = 0$, $R = r$, hence $\xi(0) = 0$.

For small displacements we may expand this expression for R,

$$R = r + \frac{\xi(t)}{r^2} + O(\xi^2) \tag{41}$$

which from comparison with the above yields.

$$u(r,t) = \frac{\xi(t)}{r^2}. \tag{42}$$

(I) Hydrodynamic

Differentiating with respect to t , the equation

$$R = \left[r^3 + 3\xi(t)\right]^{1/3}$$

we obtain

$$\frac{\partial R}{\partial t} = \frac{\dot{\xi}(t)}{R^2} \qquad 43$$

and

$$\frac{\partial^2 R}{\partial t^2} = \frac{R^3\ddot{\xi}(t) - 2[\dot{\xi}(t)]^2}{R^5}$$

$$= \frac{\ddot{\xi}(t)}{R^2} - 2\frac{[\dot{\xi}(t)]^2}{R^5} \qquad 44$$

On substituting in the momentum equation

$$\frac{\partial p}{\partial R} = -\rho\left[\frac{\ddot{\xi}(t)}{R^2} - 2\frac{[\dot{\xi}(t)]^2}{R^5}\right] \qquad 45$$

i.e.

$$p = \rho\left[\frac{\ddot{\xi}(t)}{R} - \frac{1}{2}\frac{[\dot{\xi}(t)]^2}{R^4} + \xi_1(t)\right] \qquad 46$$

The boundary condition $\underset{R\to\infty}{Lt}\ p \to 0$, gives $\xi_1(t) = 0$. At $R = a$, we will consider the pressure to be given, and that it is of the form $p = -p(t)$; then on substitution in the above, we have

$$\ddot{\xi}(t) - \frac{1}{2a^3}[\dot{\xi}(t)]^2 - a\frac{p(t)}{\rho} = 0 \qquad 47$$

where $a = [a_0^3 + 3\xi(t)]^{1/3}$

For stationary, unstressed initial conditions,

at $t = 0, \; p = 0, \; \ddot{\xi}(0) = \dot{\xi}(0) = 0$.

Transforming the variables to

$$a = [a_0^3 + 3\xi(t)]^{1/3}$$

then

$$[\ddot{a}a + 2\dot{a}^2] - \frac{1}{2a^3} a^3 \dot{a}^2 - \frac{p(t)}{\rho} = 0 \qquad 48$$

$$\ddot{a}a + 2\dot{a}^2 - \frac{1}{2}\dot{a}^2 - \frac{p(t)}{\rho} = 0$$

i.e.

$$\ddot{a}a + \frac{3}{2}\dot{a}^2 - \frac{p(t)}{\rho} = 0 \qquad 49$$

with the initial conditions

$$t = 0, \; \dot{a}(0) = 0, \text{ and } \ddot{a}(0) = 0.$$

Multiplying through by $2a^2\dot{a}$ and integrating

$$a^3\dot{a}^2 = 2\int_{a_0}^{a} \frac{p(t)}{\rho} a^2 \, da \qquad 50$$

For a step function input $p = -p(t) = -p_0 H(t)$,

where p_0 is given by the steady state theory, , we have

on integrating the right hand side,

$$\dot{a}^2 = \frac{2}{3}\left[\frac{p_0}{\rho}\right]\left\{1 - \frac{a_0^3}{a^3}\right\} \qquad 51$$

If we had the initial value $a_0 = 0$, then

$$a = \left[\frac{2}{3}\frac{p_0}{\rho}\right]^{1/2} t. \qquad 52$$

i.e.

$$f(t) = \frac{1}{3}\left[\frac{2}{3}\frac{p_0}{\rho}\right]^{3/2} t^3 \qquad 53$$

Hence

$$\dot{f}(t) = \left[\frac{2}{3}\frac{p_0}{\rho}\right]^{3/2} t^2$$

$$\ddot{f}(t) = 2\left[\frac{2}{3}\frac{p_0}{\rho}\right]^{3/2} t.$$

from which

$$p = \rho\left\{2\left[\frac{2}{3}\frac{p_0}{\rho}\right]^{3/2}\left(\frac{t}{R}\right) - \frac{1}{2}\left[\frac{2}{3}\frac{p_0}{\rho}\right]^{3}\left(\frac{t}{R}\right)^4\right\}$$

$$= \rho\left[\frac{2}{3}\frac{p_0}{\rho}\right]^{3/2}\left\{2\left(\frac{t}{R}\right) - \frac{1}{2}\left[\frac{2}{3}\frac{p_0}{\rho}\right]^{3/2}\left(\frac{t}{R}\right)^4\right\} \qquad 54$$

For a rectangular pulse of duration t', the pressure p may be obtained by superimposing a second step of opposite amplitude at a later time t'. Thus

$$a = g(t) - g(t - t')$$

where

$$g(t) = \left[\frac{2}{3}\frac{p_0}{\rho}\right]^{1/2} t.$$

hence the pressure p. .

(II) Elastic

The equations for the spherically symmetric incompressible media is

$$\rho \frac{D^2 u_R}{Dt^2} = \frac{\partial \sigma_R}{\partial R} + \frac{2}{R}(\sigma_R - \sigma_\theta) \; ; \qquad 19$$

$$\sigma_R = 2G\varepsilon_R \, , \quad \sigma_\theta = \sigma_\varphi = 2G\varepsilon_\theta \; ; \qquad 27$$

$$\varepsilon_R = \frac{\partial u_R}{\partial R} \, , \qquad \varepsilon_\theta = \varepsilon_\varphi = \frac{u_R}{R} \; ;$$

(for infinitesimal displacements) 20

For small deflections we may approximate

$$u_R = \frac{\varsigma(t)}{r^2} \simeq \frac{\varsigma(t)}{R^2} \qquad 55$$

hence

$$\varepsilon_R = -\frac{2\varsigma(t)}{R^3} \, , \quad \varepsilon_\theta = \varepsilon_\varphi = \frac{\varsigma(t)}{R^3} \qquad 56$$

Substituting in the equation of equilibrium

$$\frac{\partial \sigma_R}{\partial R} = \rho \left\{ \frac{\ddot{\varsigma}(t)}{R^2} - \frac{2[\dot{\varsigma}(t)]^2}{R^5} \right\} + 4E\frac{\varsigma(t)}{R^4} \qquad 57$$

which on integration gives

$$\sigma_R = \rho \left\{ -\frac{\ddot{\varsigma}(t)}{R} + \frac{1}{2}\frac{[\dot{\varsigma}(t)]^2}{R^4} \right\} - \frac{4}{3}E\frac{\varsigma(t)}{R^3} + \xi_2(t). \qquad 58$$

The boundary conditions are

$$(\sigma_R)_{R=a_0} + p(t) = 0 \qquad 35$$

$$\underset{R\to\infty}{\mathrm{Lt.}} (\sigma_R) \to 0 \qquad 36$$

since for elastic disturbances the first condition may be assumed to apply at the undisturbed boundary a_0 , hence

$$\ddot{\xi}(t) - \frac{1}{2a_0^3}\left[\dot{\xi}(t)\right]^2 + \frac{4}{3}\frac{E}{\rho a_0^2}\xi(t) = \frac{a_0}{\rho}p(t) \qquad 59$$

In the case of small elastic disturbance, negligible error is involved in ignoring $\left[\dot{\xi}(t)\right]^2$ term, hence, we have the much simpler equation

$$\ddot{\xi}(t) + \frac{4}{3}\frac{E}{\rho a_0^2}\xi(t) = \frac{a_0}{\rho}p(t) \qquad 60$$

Consider the response to the step function $p(t) = -p_0 H(t)$, the solution to the equation is

$$\xi(t) = A \sin \omega t + B \cos \omega t + \frac{3}{4}\frac{p_0 a_0^3}{E} \qquad 61$$

where

$$\omega^2 = \frac{4}{3}\frac{E}{\rho a_0^2} \qquad 62$$

On applying the initial conditions we obtain $A=o$, $B = -\frac{3}{4}\frac{p_o a_o^3}{E}$,
hence

$$\xi(t) = \frac{3}{4}\frac{p_o a_o^3}{E}\left(1 - \cos wt\right) \qquad 63$$

Two points of interest that should be noted are
(i) There is no evidence of the elastic wave type behaviour, a small disturbance at a_o is immediately registered at all points of medium. Thus is as a consequence of the imcompressible assumption. (ii) The solution involves undamped oscillations of $\xi(t)$ about the central value

$$\bar{\xi} = \frac{3}{4}\frac{p_o a_o^3}{E}$$

From this equation

$$\dot{\xi}(t) = \frac{3}{4}\frac{p_o a_o^3}{E} w \sin wt$$

$$\ddot{\xi}(t) = \frac{3}{4}\frac{p_o a_o^3}{E} w^2 \cos wt .$$

which will give

$$\sigma_R = \rho\left[-\frac{3}{4}\frac{p_o a_o^3}{E}\frac{w^2}{R}\cos wt + \frac{9}{32}\frac{p_o^2 a_o^6}{E^2}\frac{w^2}{R^4}\sin^2 wt\right] + p_o\frac{a_o^3}{R^3}\left(1-\cos wt\right)$$

$$= \left[-p_o\left(\frac{a_o}{R}\right)\cos wt + \frac{3}{8}\frac{p_o^2}{E}\left(\frac{a_o}{R}\right)^4\sin^2 wt + p_o\left(\frac{a_o}{R}\right)^3\left(1-\cos wt\right)\right]$$

$$= p_o\left[-\left(\frac{a_o}{R}\right)\cos wt + \left(\frac{a_o}{R}\right)^3\left(1-\cos wt\right) + \frac{3}{8}\frac{p_o}{E}\left(\frac{a_o}{R}\right)^4\sin^2 wt\right] \qquad 64$$

$$\sigma_\theta = \sigma_\varphi = \frac{p_o}{2}\left[\left(\frac{a_o}{R}\right)\cos wt - \left(\frac{a_o}{R}\right)^3\left(1-\cos wt\right) - \frac{3}{8}\frac{p_o}{E}\left(\frac{a_o}{R}\right)^4\sin^2 wt\right] \qquad 65$$

For a rectangular pulse of duration t' , the stresses will be given by

$$\sigma = g(t) - g(t-t') \qquad 66$$

where

$$g_R(t) = p_0\left[-\left(\frac{a_0}{R}\right)\cos\omega t + \left(\frac{a_0}{R}\right)^3(1-\cos\omega t) + \frac{3}{8}\frac{p_0}{E}\left(\frac{a_0}{R}\right)^4\sin^2\omega t\right]$$

The elasticity approximation remains valid for an elastic-plastic material until the stress system violates the yield criterion, i.e. for both von Mises and Tresca yield condition

$$\sigma_\theta - \sigma_R = Y \qquad 67$$

i.e. $$\xi(t) = \frac{Y R_0^3}{2E} \qquad 68$$

where R_0 is the smallest possible value for R to satisfy the yield condition. For non-vanishing R_0 therefore, $\xi(t)$ must attain a non-zero value before plastic deformation ensues. For the condition $\xi(0) = \dot{\xi}(0) = 0$, i.e. prior to $t = 0$, the medium is at rest and stress free, it follows, irrespective of the disturbance, that instantaneous plasticity is not possible, except for $R_0 = 0$.

In the case $p_0/Y \gg 1$, we can approximate $\xi(t)$ for small t

$$\xi(t) = \frac{a_0 p_0}{2\rho} t^2 \qquad 69$$

Yielding begins at $t = t_1$, at the smallest value of R i.e. a_0 ,

$$\frac{a_0 p_0}{2\rho} t_1^2 = \frac{Y a_0^3}{2E}$$

$$t_1^2 = \frac{Y}{E} \frac{\rho a_0^2}{p_0} \qquad 70$$

At this time

$$a = \left(a_0^3 + \frac{3Y}{2E} a_0^3 \right)^{1/3}$$

$$= a_0 \left(1 + \frac{3Y}{2E} \right)^{1/3} \qquad 71$$

and

$$\dot{s}(t_1) = \frac{a_0 p_0}{\rho} t_1$$

$$= a_0^2 \left[\frac{Y}{E} \frac{p_0}{\rho} \right]^{1/2} \qquad 72$$

(III) Elastic-Plastic.

Using the yield condition, and the expression for $\frac{D^2 u_R}{Dt^2}$, we have, on substitution in the equation of equilibrium.

$$\frac{\partial \sigma_R}{\partial R} = \frac{2Y}{R} + \rho \left\{ \frac{\ddot{s}(t)}{R^2} - \frac{2[\dot{s}(t)]^2}{R^5} \right\} \qquad 73$$

i.e.

$$\sigma_R = 2Y \log R + \rho \left\{ -\frac{\ddot{s}(t)}{R} + \frac{1}{2}\frac{[\dot{s}(t)]^2}{R^4} \right\} + \xi_3(t) \qquad 74$$

Consider the case where the internal pressure $p(t)$ at some time t_1, induces plasticity at the internal boundary $R = a_0$. Subsequent to t_1, the situation corresponds to

Elastic-Plastic region $\quad a \leq R \leq c(t)$

Elasitc region $\quad c(t) \leq R \leq \infty$

where $c(t)$ is the moving boundary. In these two regions the equations are

$a \leq R \leq c$

$$\sigma_R = 2Y \log R + \rho \left[-\frac{\ddot{s}(t)}{R} + \frac{1}{2}\frac{[\dot{s}(t)]^2}{R^4} \right] + \xi_3(t) \qquad 75$$

$$\sigma_\theta - \sigma_R = Y \qquad 67$$

$\dot{c} \leq R \leq \infty$

$$\sigma_R = -\frac{4E\, s(t)}{R^3} + \rho \left[-\frac{\ddot{s}(t)}{R} + \frac{1}{2}\frac{[\dot{s}(t)]^2}{R^4} \right] + \xi_2(t) \qquad 58$$

$$\sigma_\theta - \sigma_R = \frac{2E\, s(t)}{R^3}$$

(E=3G for incompressible media) 59

For the elastic region we have $\xi_2(t) = 0$, since $\underset{R \to \infty}{Lt} (\sigma_R) \to 0$

The other boundary conditions are at R=c. Since ρ is a constant, and $\dot{u}_R$ is continuous, it follows from the Rankine-Hugoniot condition that σ_R is continuous, hence σ_θ is continuous. (This is derived fromthe yield condition). These boundary conditions may be expressed

$$\frac{2E\,\varsigma(t)}{c^3} = Y \qquad 76$$

and

$$\xi_3(t) = -\frac{4E\,\varsigma(t)}{3c^3} - 2Y\log c \qquad 77$$

Finally at R = a,

$$-p(t) = 2Y\log\frac{a}{c} + \rho\left[-\frac{\ddot{\varsigma}(t)}{a} + \frac{1}{2}\frac{[\dot{\varsigma}(t)]^2}{a^4}\right] - \frac{4E\,\varsigma(t)}{3c^3} \qquad 78.$$

where

$$a = (a_0^3 + 3\varsigma)^{1/3} \qquad 79$$

and

$$c = \left(\frac{2E\varsigma}{Y}\right)^{1/3} \qquad 80$$

The boundary conditions for the solution of the above equation are obtained from the condition that $\varsigma(t)$ and $\dot{\varsigma}(t)$ are continuous at the elastic-plastic and elastic boundary,

$$t = t_1\ ; \quad \varsigma(t_1) = \frac{Y a_0^3}{2E}\ , \quad \dot{\varsigma}(t_1) = \dot{\varsigma}_1 \qquad (68)\,(72)$$

Transforming the dependent variable from $\varsigma(t)$ to

$$a = (a_0^3 + 3\varsigma)^{1/3} \qquad 79$$

we obtain

$$\rho\left\{a\ddot{a} + \frac{3}{2}\dot{a}^2\right\} + \frac{2Y}{3}\left[1 + \log\frac{2E}{3Y} + \log\left\{\frac{a^3 - a_0^3}{a^3}\right\}\right] = p(t) \qquad 80$$

for which the transformed boundary conditions are

$$t = t_1 \; ; \quad a_1 = a_0\left(1 + \frac{3Y}{2E}\right)^{1/3} ; \quad \dot{a}_1 = \frac{\dot{S}(t_1)}{a_0^2\left(1 + 3Y/2E\right)^{2/3}} = \frac{\dot{S}(t_1)}{a_1^2}$$

(71) (81)

Substituting $p_0 H(t)$ for $p(t)$, multiplying through by $2\dot{a}a^2$ and integrating, we have

$$\rho\left[a^3\dot{a}^2\right]_{a_1}^{a} + \frac{2Y}{3}\left[1 + \log\frac{2E}{3Y}\right]\left[\frac{2}{3}a^3\right]_{a_1}^{a}$$

$$+ \frac{2Y}{3}\left[\frac{2}{3}(a^3 - a_0^3)\log(a^3 - a_0^3) - \frac{2}{3}a^3\log a^3\right]_{a_1}^{a} = \frac{2}{3}p_0\left[a^3\right]_{a_1}^{a}$$

$$t_1 \leq t \leq t' \qquad 82$$

which reduced to

$$\rho\left[a^3\dot{a}^2 - a_1^3\dot{a}_1^2\right] + \frac{4Y}{9}\Big\{(a^3 - a_1^3)\left(1 + \log\frac{2E}{Y}\right) + (a^3 - a_0^3)\log(a^3 - a_0^3)$$

$$- (a_1^3 - a_0^3)\log(a_1^3 - a_0^3) - a^3\log a^3 + a_1^3\log a_1^3\Big\}$$

$$= \frac{2}{3}p_0(a^3 - a_1^3) \qquad 83$$

Transforming the independent variable from a to x , where

$$a = a_1 (1 + x)^{1/3} \tag{84}$$

we obtain

$$\rho \left[\frac{a_1^5 \dot{x}^2}{9(1+x)^{1/3}} - a_1^3 \dot{a}_1^2 \right] + \frac{4Y}{9} \Big\{ a_1^3 x \left(1 + \log \frac{2E}{3Y}\right)$$

$$+ \left[a_1^3 (1+x) - a_0^3 \right] \log \left[a_1^3 (1+x) - a_0^3 \right] - (a_1^3 - a_0^3) \log (a_1^3 - a_0^3)$$

$$- a_1^3 (1+x) \log a_1^3 (1+x) + a_1^3 \log a_1^3 \Big\} = \frac{2}{3} p_0 a_1^3 x \tag{85}$$

Using $a_1 = a_0 \left(1 + \frac{3Y}{2E}\right)^{1/3}$, and neglecting higher order terms in (Y/E), this reduces to

$$\rho a_1^2 \left[\dot{x}^2 (1+x)^{-1/3} - \dot{x}_1^2 \right] + 4Y \Big\{ x \Big[1 + \log\left(\frac{2E}{3Y}\right) + \log\left(\frac{x + \frac{3Y}{2E}}{1+x}\right) \Big]$$

$$+ \frac{3Y}{2E} \log \left[1 + \frac{2Ex}{3Y} \right] - \log (1+x) \Big\} = 6 p_0 x . \tag{86}$$

and the boundary conditions now becomes

$$x = 0 \qquad \dot{x}(t_1) = \frac{3\dot{a}_1}{a_1} \approx \frac{3}{a_1} \left\{ \frac{Y p_0}{E \rho} \right\}^{1/2} \tag{87}$$

The complete integration may be effected numerically.

Consider the case when $a_0 = 0$; as pointed out earlier this permits instantaneous plasticity. The equation reduces to

$$\rho \left\{ a \ddot{a} + \frac{3}{2} \dot{a}^2 \right\} + \frac{2Y}{3} \left\{ 1 + \log \frac{2E}{3Y} \right\} = p(t) \tag{88}$$

$$\rho\left\{a\ddot{a} + \frac{3}{2}\dot{a}^2\right\} = p(t) - p_s \tag{89}$$

where

$$p_s = \frac{2Y}{3}\left[1 + \log\frac{2E}{3Y}\right] \tag{90}$$

The boundary conditions $\xi(0) = \dot{\xi}(0) = 0$ at $t=0$ becomes

$$a = 0 \qquad a^2\dot{a} = 0 \qquad t = 0 \tag{91}$$

A finite $\dot{a}(0)$ makes the second equation redundant, this difficulty is resolved by imposing that $\dot{a}(0)$ be non-infinite for finite pressure pulses. The condition insures the vanishing of $\dot{a}(0)$ for $p(t) = p_o H(t)$

Multiphy the equation by $2a^2\dot{a}$ and integrating

$$\rho a^3\dot{a}^2 - \rho a^3(0)\dot{a}^2(0) = 2\int_0^a [p(t) - p_s]\, a^2\, da \tag{92}$$

which for

$$a^3(0)\,\dot{a}^2(0) = 0$$

reduces to

$$\rho a^3\dot{a}^2 = 2\int_0^a [p(t) - p_s]\, a^2\, da \tag{93}$$

Substituting $p_o H(t)$ for $p(t)$, $p_o > p_s$, we have

$$\dot{a}^2 = \frac{2}{3}\,\frac{p_o - p_s}{\rho} \tag{94}$$

i.e.

$$a = \left\{\frac{2}{3}\,\frac{(p_o - p_s)}{\rho}\right\}^{1/2} t. \tag{95}$$

From this

$$\xi(t) = \frac{1}{3}\left\{\frac{2}{3}\frac{(p_o - p_s)}{\rho}\right\}^{3/2} t^3 \qquad 96$$

$$c = \left\{\frac{2E}{3Y}\right\}^{1/3}\left\{\frac{2}{3}\frac{(p_o - p_s)}{\rho}\right\}^{1/2} t. \qquad 97$$

$$\dot{\xi}(t) = \left\{\frac{2}{3}\frac{(p_o - p_s)}{\rho}\right\}^{3/2} t^2$$

and

$$\ddot{\xi}(t) = 2\left\{\frac{2}{3}\frac{(p_o - p_s)}{\rho}\right\}^{3/2} t .$$

hence

$$\sigma_R = 2Y \log\frac{R}{c} - \frac{2Y}{3} + \rho\left\{-\frac{\ddot{\xi}(t)}{R} + \frac{1}{2}\frac{[\dot{\xi}(t)]^2}{R^4}\right\} \qquad 98$$

and

$$\sigma_\theta = Y + \sigma_R \qquad 67$$

As before, for a rectangular pulse of duration t', the stresses may be obtained by superimposing a second step of opposity amplitude at a later time t'.

CHAPTER 3

EXPERIMENTAL METHODS

In order to obtain a comparison between theory and results obtained in practice, it was decided to carry out some experimental work. Of necessity, this had to be a simple experiment which did not involve a great deal of instrumentation. It was decided to find the extend of the plastic zone in a target material due to impact by a 1/8 in diameter ball bearing. This required a high velocity gun and a velocity measuring device, both of which were available in the laboratory.

Two experimental methods may possibly be used for determining the deformation of the metal after impulsive loading, namely (I) a metallographic etching technique, and (II) micro-hardness technique.

Four metallographic techniques may be used to detect the extent of the deformation in the interior of a semi-infinite specimen. There are three techniques for specimens which more closely approach the ideal rigid-plastic material.

One method uses Austenitic Manganese Steel, heat treated by holding at 1,100°F for 30 min and quenching in water. A strain free surface is then produced by grinding, polishing, and etching. The etching cycle is as follows: Etch 15 sec in 3% nital, rinse in ethyl alcohol, etch 15 sec in 10% H Cl in alcohol, rinse 15 sec in ethyl alcohol. This is usually repeated three times, followed by 15 sec in 2% ammonium Hydroxide in alcohol, and rinsing in ethyl alcohol. The polished and etched face must be protected carefully from corrosion particularly in humid atmosphere. Transformation of austenite to martensite is produced by deformation, which results in the appearance of slip lines. The magnetic nature of these lines can be demonstrated by a special colloid pattern technique. The polished surface of the specimen is covered with a thin colloidal suspension of magnetic particles, application of a magnetic field will cause a visible concentration of the colloid over the magnetic areas.

For metallographic purposes a drop of the magnetic solution is placed on the polished specimen and covered with a microscope cover glass. In the field of the magnet concentrations of the colloid particles will delineate the magnetic phases.

The second is for a mild steel specimen, here the section is etched in Fry's reagent which preferentially darkens plastically deformed zones. Only certain batches of steel respond satisfactorily to this treatment, a highly sensitive steel is one that contains 0.20% carbon, 0.52% manganese, and other elements less than 0.05%. The third metallographic technique is based on carbide precipitation described by Wilson[48]. In this case the material is a 0.7% carbon steel which is water quenched from 800°C. After impact it is tempered at 200°C for 15 min. The specimen is then sectioned, polished and etched in nital which shows the plastically strained material as a light etching zone.

For 70:30 brass metallographic techniques are available with which deformation can be detected with a very high sensitivity. Specimens are annealed at 600°C for 2 hrs establishing a grain size of 0.05 mm diameter; a grain size of this order is desirable to facilitate metallographic observations.

The test surface was prepared on abrasive papers to remove all evidence of surface grain-rumpling, and then metallographically polished to remove the surface deformation produced during the abrasion method. Finally it was etched to develop the metallographic indications of deformation. The etch used was an ammonium hydroxide-hydrogen peroxide reagent. (Ammonium hydroxide 1 volume, hydrogen peroxide (3%) 2 volumes, and water 1 volume); this was applied by swabbing. Previous investigators (Samuels)[50] have found that this etch will give indications of deformation of less than 0.1% in compression. The boundaries determined from this process may be taken as boundaries of constant strain, because the development of the etching effects indicates that a more or less definite amount of slip has occurred in the grain concerned.

The metallographic methods have the advantage that they allow examination of the strain in a semi-infinite block. They have the disadvantage that it is only possible to determine one contour of uniform strain, and it is difficult to ascribe a definite magnitude of this strain.

Information regarding the distribution of stress that existed in an impulsively loaded body, can be obtained by plotting contours of equal hardness on sections of the body. Only qualitative results can be obtained and they depend on good hardening characteristics of the target material, otherwise small error in readings (which can easily occur from the uncertainty of the outline of the impression) or localized effects, e.g. cracks, will cancel out any variation that might have existed.

CHAPTER 4

RESULTS

The pressure produced by impact is given by

$$p_o = \frac{1}{2} \frac{\lambda \rho_p \rho_t}{\left[(\lambda \rho_p)^{1/2} + (\rho_t)^{1/2}\right]^2} V^2 \qquad 33$$

and this is sustained during the penetration which is completed in time t', where

$$t' = \frac{d}{V}\left\{1 + \left(\frac{\lambda \rho_p}{\rho_t}\right)^{1/2}\right\} \qquad 34$$

Penetration will proceed at a velocity U,

$$U = \frac{V}{1 + \left(\frac{\rho_t}{\lambda \rho_p}\right)^{1/2}} \qquad 99$$

and the depth of penetration, which is independent of the velocity of impact, (providing that this is high enough for us to assume the applicability of the hydrodynamic theory) is given by

$$\delta = d\left(\lambda \rho_p / \rho_t\right)^{1/2} \qquad 1$$

The final diameter of the crater at the level of the original surface is

$$D = \frac{dV}{\left(\frac{1}{\rho_t}\right)^{1/2} + \left(\frac{1}{\lambda \rho_p}\right)^{1/2}} \cdot \frac{1}{(2Y)^{1/2}} \qquad 2$$

Since the spherical projectile is capable of sustaining an internal pressure, we will take $\lambda = 1$. Measured quantities for the spherical projectile and the 70:30 brass are:

$d = 0.125$ ins

$\rho_p = 0.238$ lb/in^3

$\rho_t = 0.309$ lb/in^3

$Y_s = 13{,}600$ p.s.i.

$E = 15{,}400{,}000$ p.s.i.

The calculated values for the pressure, time of penetration, velocity of penetration, depth of penetration, and final diameter of the crater are tabulated for impact velocities from 3500 ft/sec to 7,000 ft/sec. Plots of these values are shown in figs. 2, 3, and 4, as well as the measured values for the depth of penetration and diameter of the crater.

V (ft/sec)	3500	4000	5000	6000	6500	7000
t' (sec)	5.60×10^{-6}	4.90×10^{-6}	3.92×10^{-6}	3.27×10^{-6}	3.01×10^{-6}	2.80×10^{-6}
U (ft/sec)	1640	1870	2340	2800	3050	3280
p_o (p.s.i)	0.157×10^{6}	0.205×10^{6}	0.320×10^{6}	0.461×10^{6}	0.541×10^{6}	0.628×10^{6}
δ (ins.)	0.110	0.110	0.110	0.110	0.110	0.110
D (ins.)	0.42	0.48	0.60	0.72	0.78	0.84

The measured values were as follows:

V (ft/sec)	3920	4920	5310	5660	6120	6590
δ (ins)	0.115	0.140	0.140	0.155	0.155	0.160
D (ins)	0.200	0.230	0.240	0.250	0.275	0.275
c (ins).	0.235	0.245	0.250	0.265	0.285	0.295

4.1 Calculation of the Extreme Radii of the Elastic-Plastic Boundary

The hydrodynamic theory will not give us an estimate of the plastic zone as the yield condition is independent of the hydrostatic pressure. In view of this we can only consider the elastic and elastic-plastic solution for comparison with the measured values.

(i) Elastic

It was stated earlier that under dynamic loading the elastic equations will hold for stresses which violate the static yield condition. Kumar[29] has pointed out

70:30 BRASS (Annealed at 1100°F for 2 hrs.)

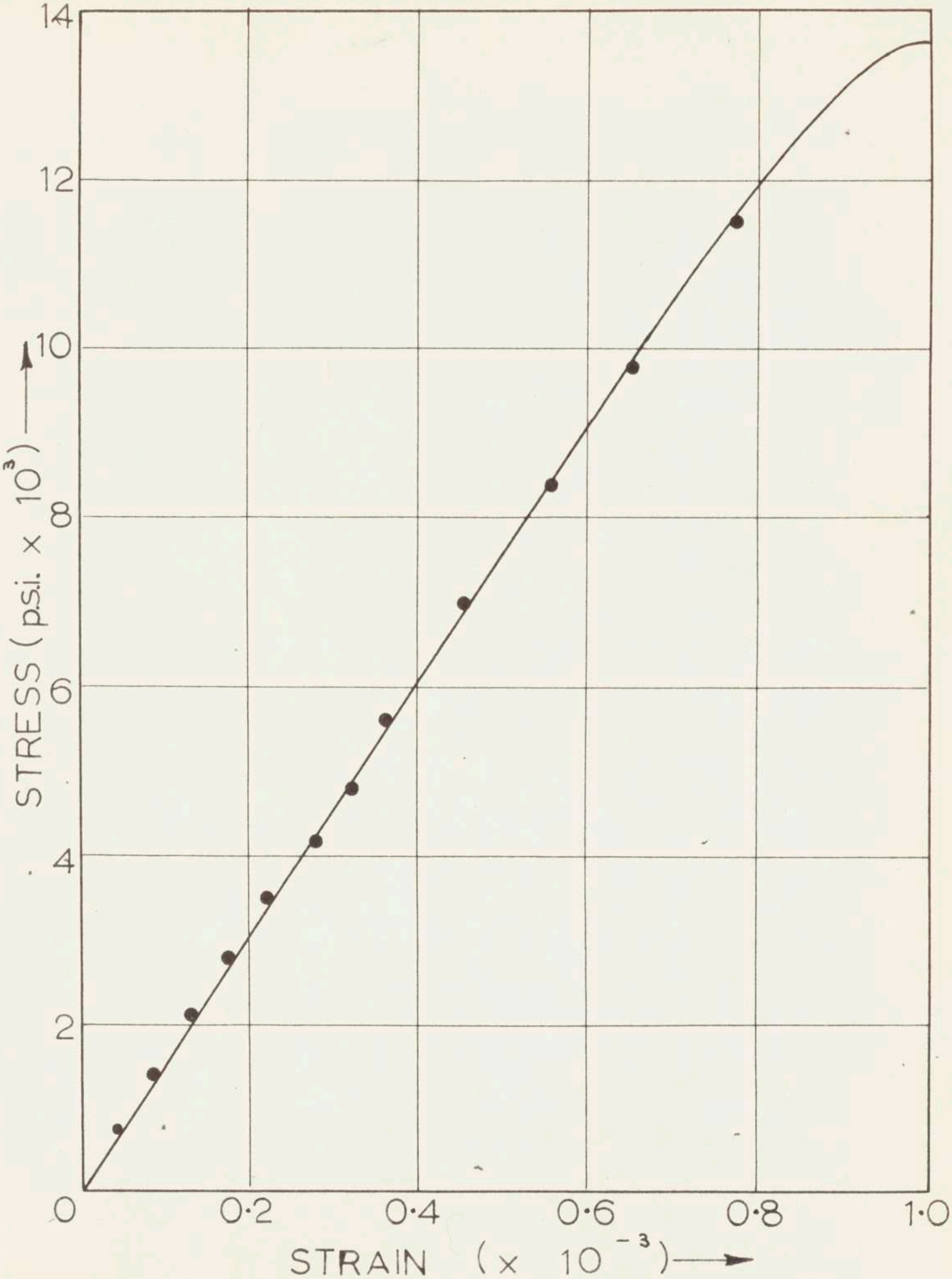

FIG. 1 STATIC STRESS STRAIN.

FIG. 2. PENETRATION PRESSURE, TIME & VELOCITY.

70:30 BRASS TARGET; STEEL PROJECTILE.

FIG. 3 DEPTH of CRATER.

70:30 BRASS TARGET; STEEL PROJECTILE.

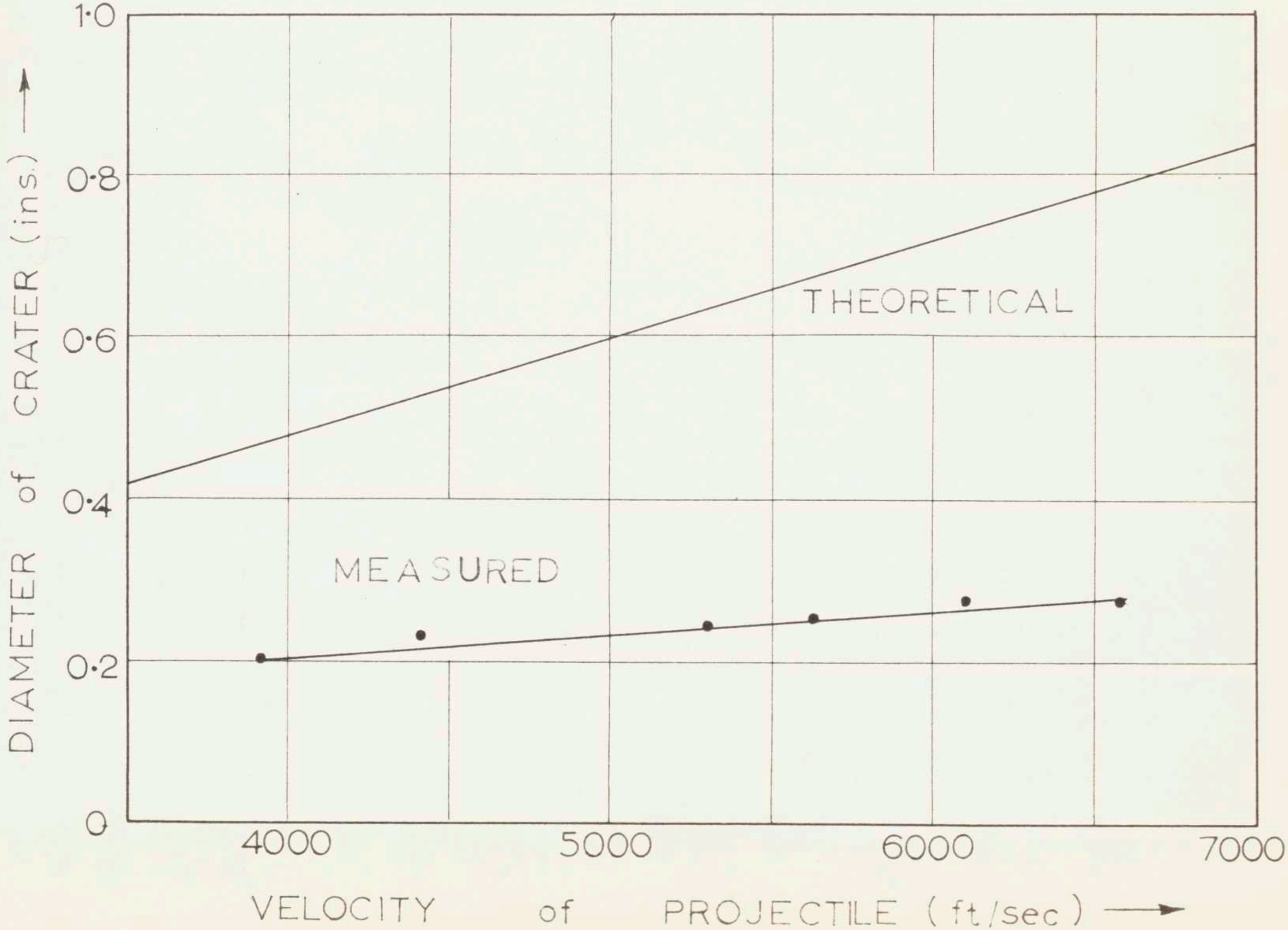

FIG. 4 FINAL DIAMETER of CRATER.

that for many materials the plastic part of the stress-strain curve tends to become closer and closer to the continuation of the elastic straight line as the rate of loading becomes larger and larger. Thus; for extremely high rates of loading it might be assumed that the stress-strain curve is linear up to fracture. Assuming that the elastic equations hold above yield, we may estimate the extent of the plastic zone from the solution given by these equations.

The expressions for σ_R and σ_θ are

$$\sigma_R = -p_0\left[\left(\frac{d}{2R}\right)\cos\omega t - \left(\frac{d}{2R}\right)^3(1-\cos\omega t) - \frac{3}{8}\frac{p_0}{E}\left(\frac{d}{2R}\right)^4\sin^2\omega t\right] \qquad 64.$$

$$\sigma_\theta = \frac{p_0}{2}\left[\left(\frac{d}{2R}\right)\cos\omega t - \left(\frac{d}{2R}\right)^3(1-\cos\omega t) - \frac{3}{8}\frac{p_0}{E}\left(\frac{d}{2R}\right)^4\sin^2\omega t\right] \qquad 65$$

hence the yield condition is

$$\frac{3}{2}p_0\left[\left(\frac{d}{2R}\right)\cos\omega t - \left(\frac{d}{2R}\right)^3(1-\cos\omega t) - \frac{3}{8}\frac{p_0}{E}\left(\frac{d}{2R}\right)^4\sin^2\omega t\right] = Y. \qquad 100$$

On the addition of a negative pressure p_0 after time t', the magnitude of the resulting wave will be diminished as the phase difference is small (0.729 radius is the max.).

Since the stress magnitude is diminished on application of the negative pressure, the minimum value of $\left(\frac{d}{2R}\right)$ will occur in the interval $0 - t'$. We can clearly see from the above expression that this occurs at $t = 0$, i.e.

$$c = \frac{3}{2} \frac{p_0}{Y} a_0 \qquad 101$$

Values of c for different values of $\frac{Y_s}{Y} a_0$ and impact velocities in the range 3500 ft/sec to 7000 ft/sec are tabulated below, Y is the dynamic yield stress of the material. These are plotted in fig. 5, together with the measured values.

V (ft/sec)	3500	4000	5000	6000	6500	7000
c (cms) $\left\{\frac{a_0 Y_s}{Y} = \frac{1}{100}\right\}$	0.173	0.226	0.353	0.510	0.599	0.693
$\left\{\frac{a_0 Y_s}{Y}\right\} = \frac{1}{150}$	0.116	0.150	0.236	0.340	0.400	0.461
$\left\{\frac{a_0 Y_s}{Y} = \frac{1}{200}\right\}$	0.087	0.113	0.176	0.255	0.300	0.347
$\left\{\frac{a_0 Y_s}{Y} = \frac{1}{250}\right\}$	0.069	0.090	0.141	0.204	0.240	0.278

(ii) Elastic Plastic

1. $a_0 = 0$

The limit of the plastic zone at any time t will be given by

$$c = \left\{\frac{2E}{3Y}\right\}^{1/3} \left\{\frac{2}{3} \frac{(p_0 - p_s)}{\rho}\right\}^{1/2} t . \qquad 97$$

70:30 BRASS TARGET; STEEL PROJECTILE.

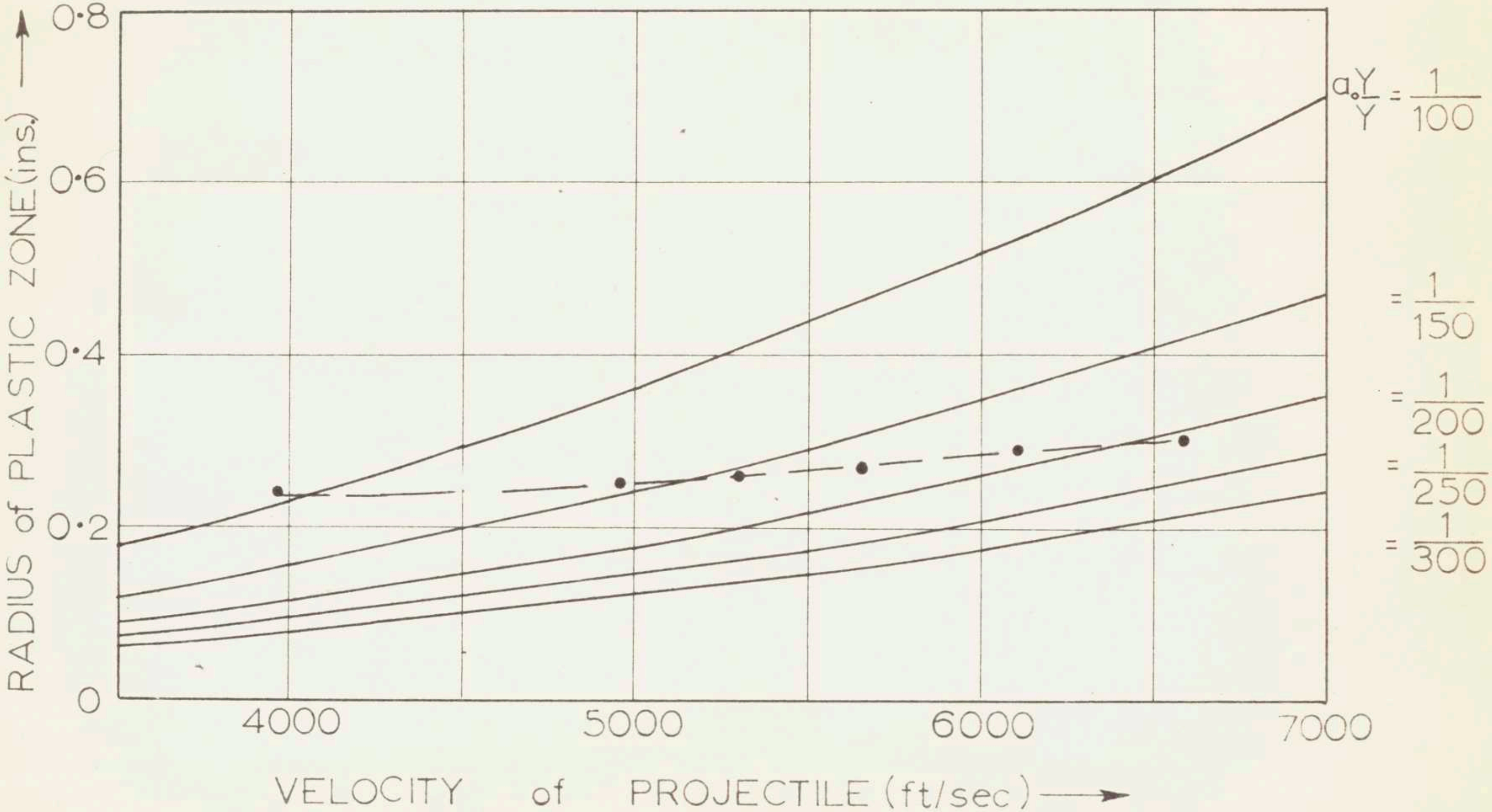

FIG. 5. MAXIMUM RADIUS of PLASTIC ZONE.(ELASTIC THEORY)

where

$$p_s = \frac{2Y}{3}\left[1 + \log \frac{2E}{3Y}\right] \qquad 90$$

For the rectangular impulse of duration t', the complete solution of C for $d\xi > 0$ is

$$C = \left\{\frac{2E}{3Y}\right\}^{1/3} \left\{\frac{2}{3} \frac{(p_0 - p_s)}{\rho}\right\}^{1/2} \left\{t - [t - t']\right\} \qquad 102$$

which gives the maximum value of c as

$$C = \left\{\frac{2E}{3Y}\right\}^{1/3} \left\{\frac{2}{3} \frac{(p_0 - p_s)}{\rho}\right\}^{1/2} t' \qquad 103$$

We note that the elastic-plastic boundary becomes stationary at the moment of the removal of the pressure.

Values of c and p_s for different values of Y and a range of impact velocities are tabulated below. These are plotted in fig. 6.

2. $a_0 \neq 0$.

The time taken for the material at the surface of the cavity to reach yield is given by

$$t_1 = 7.49 \frac{a_0}{V}\sqrt{\frac{Y}{Y_s}} \quad \times 10^{-3} \text{ sec.} \qquad 104$$

where a_0 was the original radius of the cavity expressed in inches and V the velocity of impact expressed in ft/sec. For example, let us consider the case at the velocity of impact of 7000 ft/sec assuming a yield of $4\,Y_s$; then for

V (ft/sec)	3500	4000	5000	6000	6500	7000
p_0 (p.s.i)	0.157×10^{6}	0.205×10^{6}	0.320×10^{6}	0.461×10^{6}	0.541×10^{6}	0.628×10^{6}.
t' (sec)	5.60×10^{-6}	4.90×10^{-6}	3.92×10^{-6}	3.27×10^{-6}	3.01×10^{-6}	2.80×10^{-6}.
$p_s(Y_s)$ p.s.i	0.068×10^{6}	0.068×10^{6}	0.068×10^{6}	0.068×10^{6}	0.068×10^{6}	0.068×10^{6}
c (ins)	0.426	0.460	0.501	0.522	0.530	0.535
$p_s(2Y_s)$ p.s.i.	0.138×10^{6}	0.138×10^{6}	0.138×10^{6}	0.138×10^{6}	0.138×10^{6}	0.138×10^{6}
c (ins)	0.166	0.264	0.357	0.385	0.396	0.405
$p_s(2.5Y_s)$ p.s.i	0.152×10^{6}	0.152×10^{6}	0.152×10^{6}	0.152×10^{6}	0.152×10^{6}	0.152×10^{6}
c (ins)	0.078	0.223	0.310	0.353	0.361	0.372
$p_s(3.0Y_s)$ p.s.i.		0.178×10^{6}	0.178×10^{6}	0.178×10^{6}	0.178×10^{6}	0.178×10^{6}
c (ins)	—	0.147	0.270	0.317	0.329	0.341
$p_s(3.5Y_s)$ p.s.i.		0.202×10^{6}	0.202×10^{6}	0.202×10^{6}	0.202×10^{6}	0.202×10^{6}
c (ins)	—	0.044	0.235	0.284	0.301	0.315
$p_s(4.0Y_s)$ p.s.i.			0.226×10^{6}	0.226×10^{6}	0.226×10^{6}	0.226×10^{6}.
c (ins)	—	—	0.200	0.262	0.280	0.291

$a_0 = 1/10$ in, 1/100 in and 1/1000 in yield begins after a time 0.21×10^{-6} sec, 0.021×10^{-6} sec, and 0.0021×10^{-6} sec, that is after 7.5%, 0.75% and 0.075% of the total impact time. At these times the elastic-plastic boundary for the case $a_0 = 0$ will be $c = 0.0218$, 0.00218 and 0.000218 ins. respectively. The corresponding stresses at the elastic-plastic surface will be $\sigma_R = -0.128\times10^{6}$ p.s.i and $\sigma_\theta = -0.074\times10^{6}$ p.s.i.; p is far greater than this σ_R.

70:30 BRASS TARGET ; STEEL PROJECTILE.

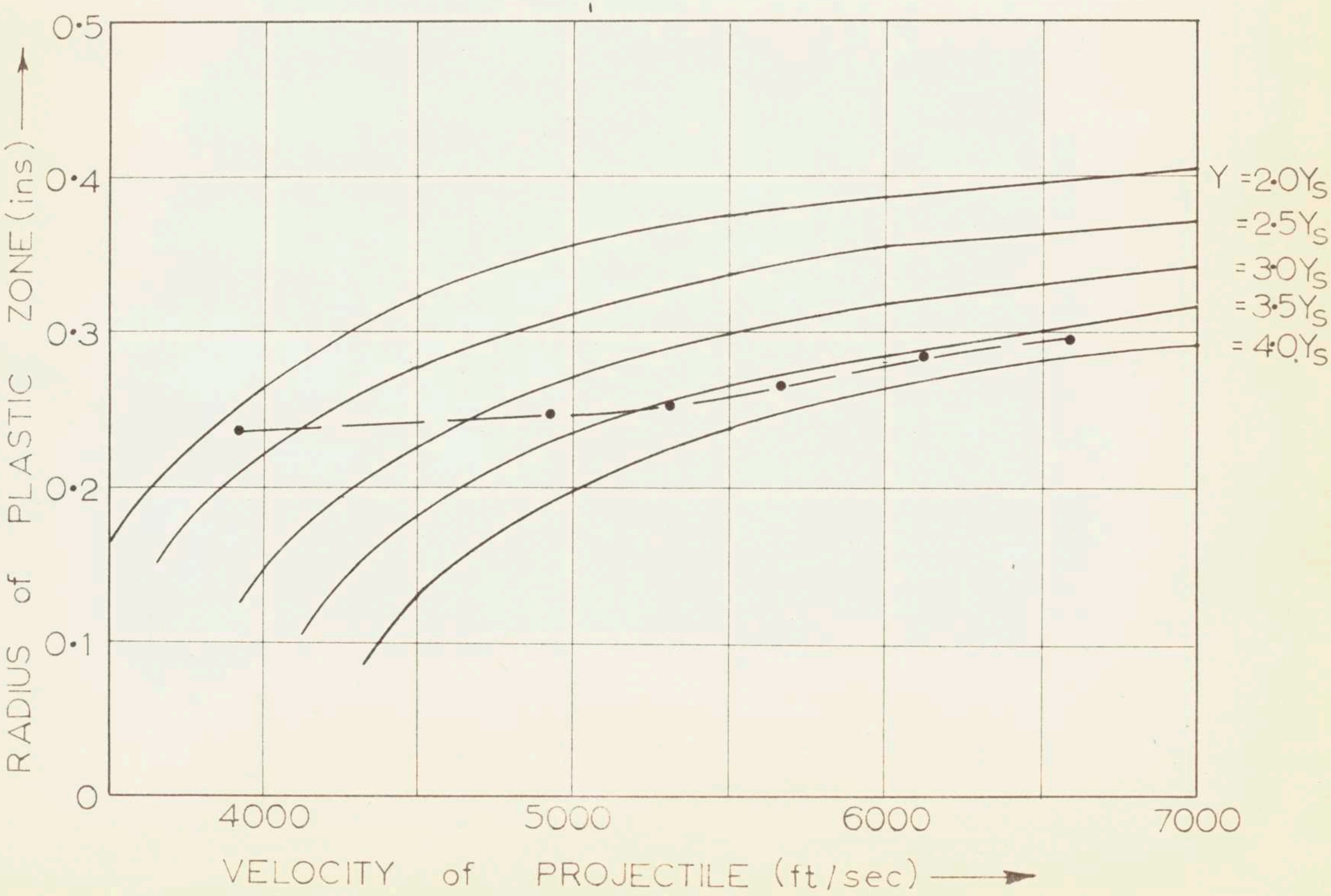

FIG. 6 MAXIMUM RADIUS of PLASTIC ZONE (PLASTIC THEORY)

When yielding begins at a_1, the velocity of the elastic-plastic boundary will be given by

$$\dot{c}_1 = \left\{\frac{2E}{3Y}\right\}^{1/3} \left\{1 + \frac{2E}{3Y}\right\}^{2/3} \dot{a}_1 \qquad 105$$

$$= 190\,\dot{a}_1$$

$$= 3\cdot 13 \times 10^5 \text{ ins/sec.}$$

This velocity is independent of the initial radius a_0. For the $a_0 = 0$, the corresponding velocity is

$$\dot{c} = 1.04 \times 10^5 \text{ in/sec.}$$

These preliminary calculations indicate that the maximum value of c would be higher for the case when $a_0 \neq 0$ than $a_0 = 0$. The measured values for c indicate that the values given by the elastic-plastic theory for $a_0 \neq 0$ would be too high to be of interest in the present problem. In view of this and the large amount of numerical calculation that would be involved in obtaining c, it was decided not to carry out the numerical integration of the differential equation in x.

4.2 Metallographic Indications.

The metallographic indications of deformation can be classified into four distinct groups, each of which are shown in figs. 7, 8, 9, and 10. These photographs were taken at increasing distances from the crater boundary. Each of these four groups were present in all target specimens, and are particularly prominent, even thought the distances between two successive groups is relatively small.

Samuel[50] has classified the four groups having the following general characteristics:

Type I. Systems of parallel grooves or lines of etch pits, orientated acoording to the crystallographic planes of the particular grains in which they occurred. Developed at low deformations. (fig. 10).

Type II. Relatively wide bands orientated similarly to those of Type I, and apparently a development of them. Developed after low to medium deformations. (Fig. 9).

Type III. Two sets of parallel lines, the orientations of which are related to the direction of compression and not to those of the grains. Developed after medium to heavy deformations. (Fig. 8).

Type IV. Two sets of parallel undulations, the orientations of which were related to the direction of compression, but at different angles to those of the Type III indications. Developed only after heavy deformations. (Fig. 7).

Figure 7 shows the grain deformation at the crater boundary. The unetched block area was the steel projectile that had melted at impact, and the grey area above, the crater formed by the impact. Comparing with fig. 10 we see that the grains were extensively

x 500

Fig. 7 Deformation of grain in the vicinity of the crater. (Type IV).

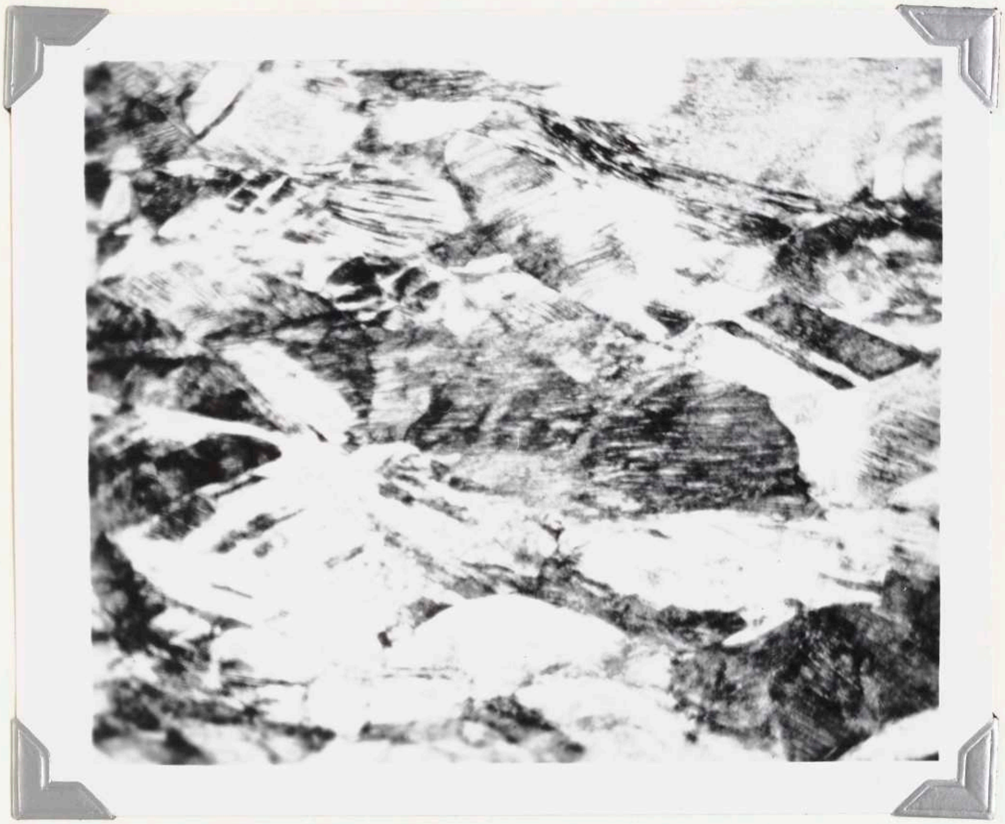

x 500

Fig. 8 Deformation of grain (Type III).

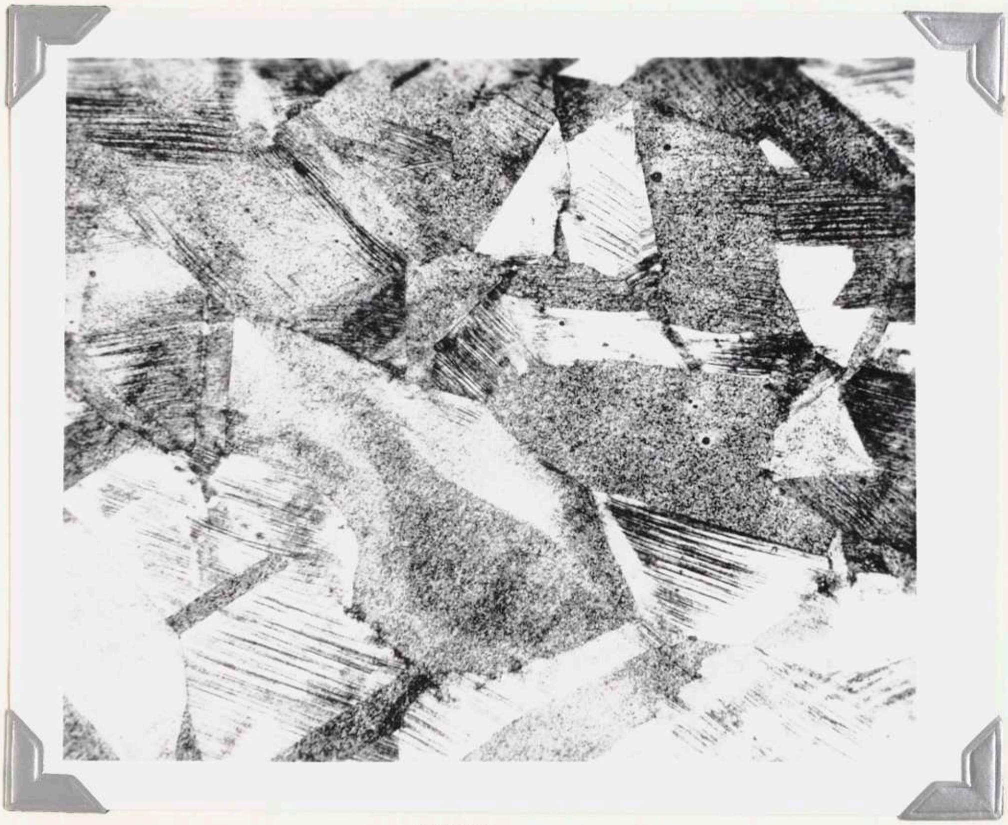

×500

Fig. 9. Deformation of grain showing etch pit lines (Type II and III).

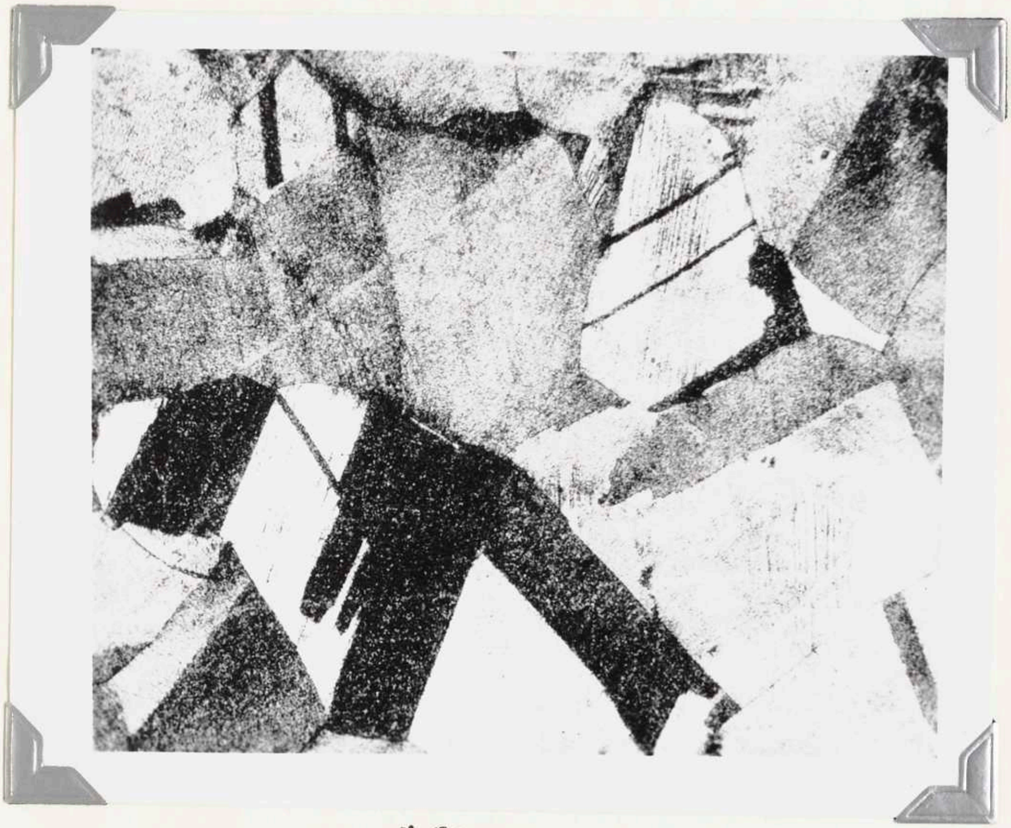

x 500

Fig. 10 Deformation of grains showing etch pit lines and deformed annealing twins (Type I).

elongated during impact, the orientation of the elongation being in the same direction as the impulsive load. Rinehart and Pearson[1] have pointed out that the tendency of the material to deform by grain flow increases with high pressure and decreases with high strain rates. In the area shown in fig. 7, the pressure would have been very high.

Figure 9 shows grains in which the etch pit lines are closely spaced, and one grain gives a good example of the etch pits in two sets of parallel lines. One is lead to conclude that these etch pits are twinnings in some grains and slip in others, since some are orientated along twin directions, while the others are not. Twins are an indication of a high rate of strain.

Figure 10 shows the structure in the less deformed grain area. Definite evidence that deformation took place are the curved annealing twins; also, the parallel etch pit lines.

CHAPTER 5

CONCLUSIONS

Experimental work was limited to the manganese steel and 70 : 30 brass targets. The reason for this was that the other steels were not available in small quantity. Furthermore, only one impact test was carried out with the Hatfield's manganese steel, because of its "commercially unmachinable"[46] properties. No comparisons with theory were made; the experimental results for the single test is presented below

5.1 Manganese Steel Target

The suspended magnetic colloid apparatus, described earlier, could not be made available. A spring-balanced suspended magnet, which works on the same principle as the magnetic colloid was tried, but was found to be not sensitive enough to determine the martensitic zone. In this case we had to resort to the micro-hardness indentation method

From the plot, fig. 11, we can see that there was a large variation in the hardness number at distances greater than 0.45 cm from the center of the crater Variations in readings at a particular

MANGANESE STEEL TARGET; STEEL PROJECTILE.

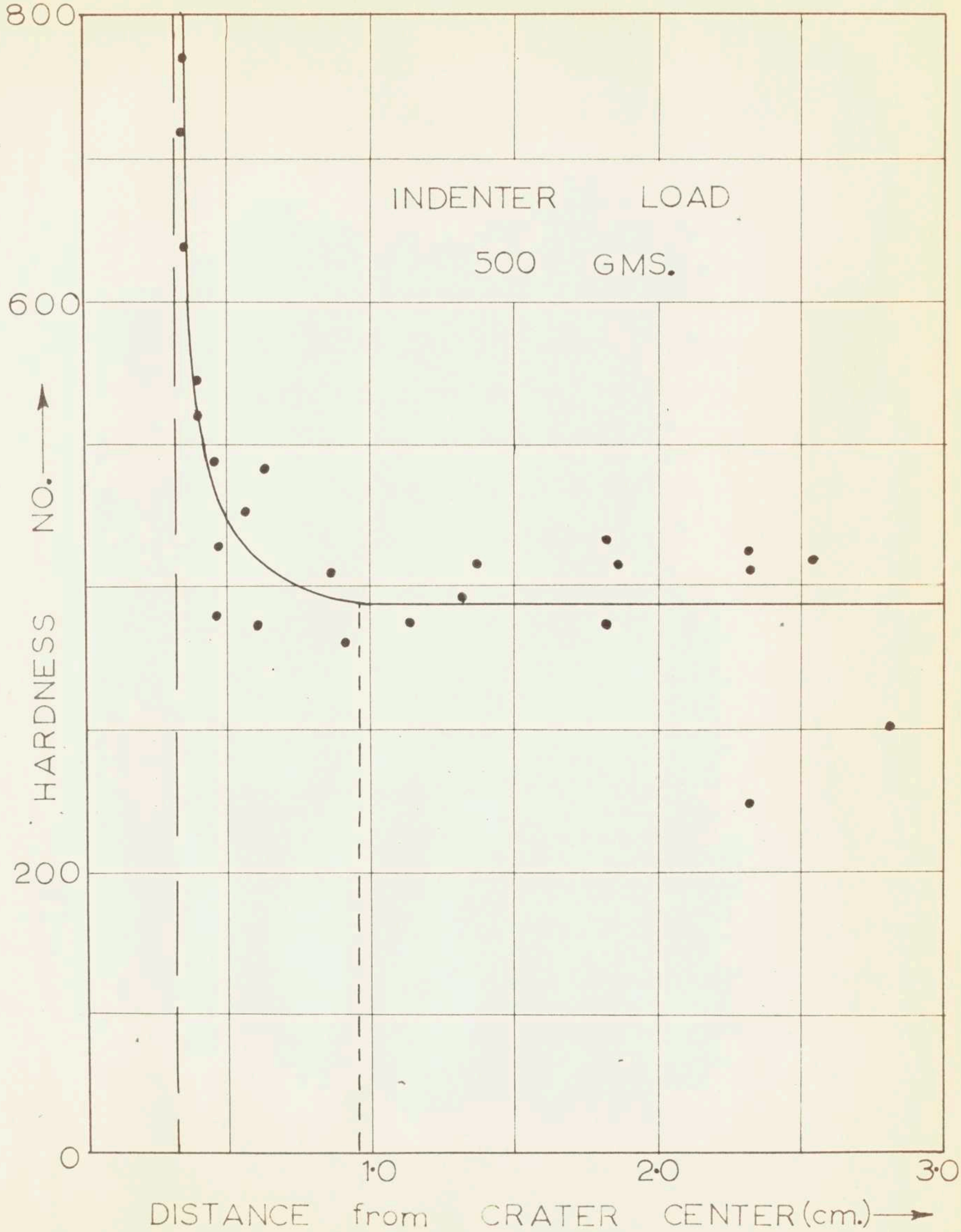

FIG. 11. DIAMOND HARDNESS TEST on TARGET.

radius precluded the drawing of iso-hardness contours. Near the crater, and approaching towards it, the hardness number increases rapidly.

The difficulty in obtaining consistent results can be put down to two causes:

(a) The hardness and work-hardening property of the manganese steel, and

(b) Surface pitting (dirty steel).

High loads had to be used in order to obtain accuracy in measuring the diaganol length of the indentation. Because of the work hardening property of the steel, this could give false readings of the hardness number. However, it should give the correct indication as to the extent of the plastic zone. In fig. 11 the radius of the plastic zone was taken to be 0.95 cm, but this could be equally well drawn to give a radius of 0.75 cm.

5.2 70: 30 Brass

Theoretical estimation of the depth of penetration and radius of the crater give a very poor comparison with the measured values. The difference must arise from strength consideration. If we take the yield for steel to be between 80,000 and 90,000 p.s.i., the impact pressure as estimated by the hydrodynamic theory, was only 2 to 8 times this value. This strength would lower the projectile's flow velocity. In this case we expect a higher penetration and a smaller crater radius, the plots bear out this conclusion. No known experimental evidence exists to compare the actual value of the penetration pressure with the theoretical estimate, and this could be the main source of error in the predictions.

5.3 Boundary of the Plastic Zone

The boundary determined by the ammonium hydroxide - hydrogen peroxide etching method may be regarded as being the elastic-plastic boundary in the sense that it is the boundary between the zones in which the slip and twinning has occurred in the majority of the grains and the zone which it has not. There was a degree of uncertainty as to the exact location of the boundary; however, the repeatability of these observations was quite good. An example are the points (all of which were the average of at least three readings) for the 5,310 ft/sec impact velocity in fig. 12. Furthermore, this boundary should not have been affected by the elastic wave reflected from the boundary of the target specimen as the time taken by the elastic wave (velocity approximately 12,000 ft/sec) to reach the boundary of the target (a cylinder radius 1 in, height 1 in) was too long (6.9×10^{-6} secs). We can deduce that the plastic wave should have a velocity of less than 1/4 the elastic wave velocity for the back of the outgoing wave to have interacted with the front of the reflected wave inside the measured plastic zone. This is lower than the expected speed of the plastic wave.

The plastic boundary obtained from the observation of the etch pit lines were found to approximately lie on a hemisphere

70:30 BRASS TARGET; STEEL PROJECTILE.

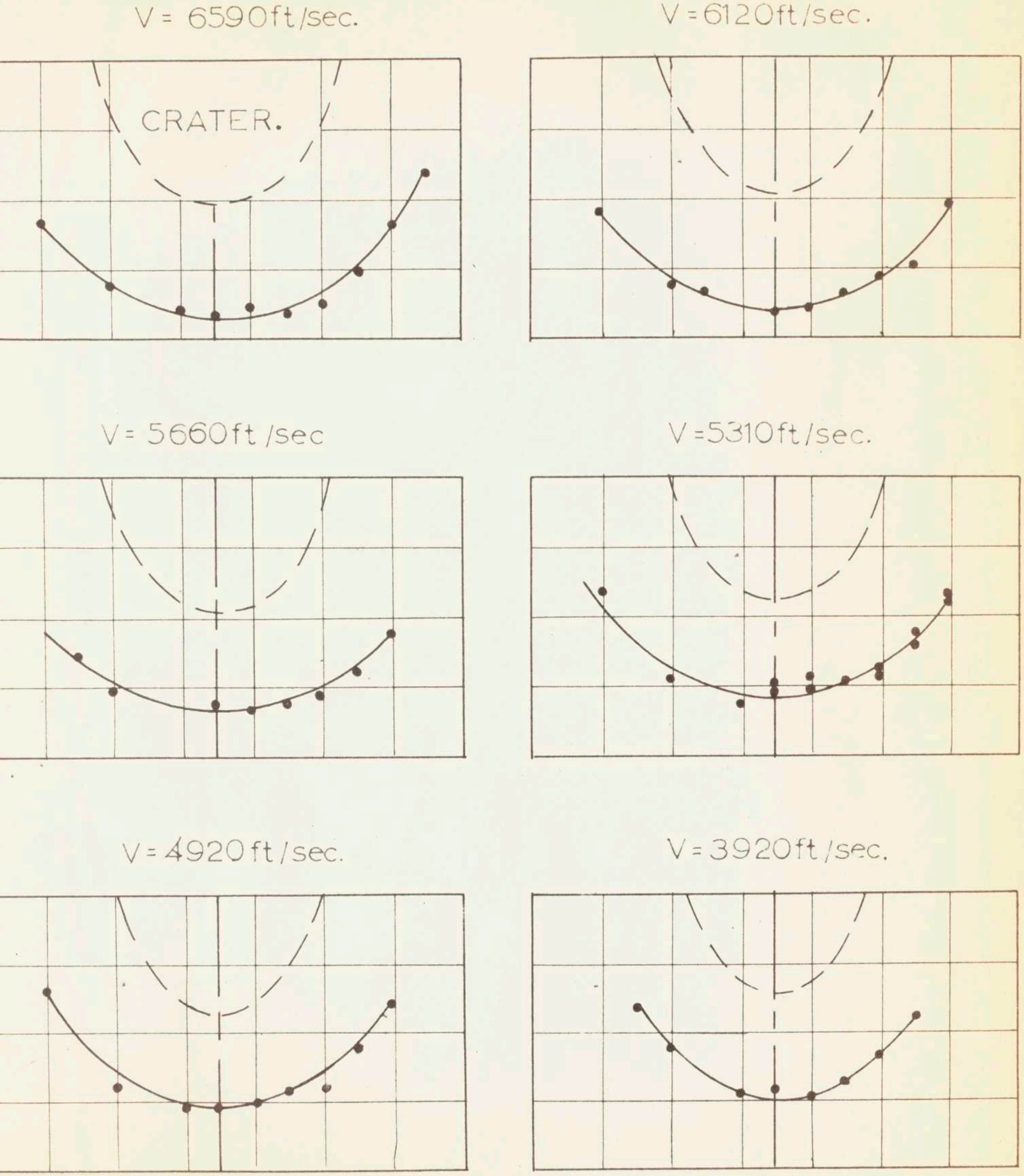

FIG. 12. MEASURED MAXIMUM ELASTIC-PLASTIC ZONE.

with the point of impact as origin, for the four highest velocities of impact. The two lower velocities gave radii which were appreciably less than the depth. In this case the radius of the plastic zone was taken as the depth to the elastic-plastic boundary at the center line of the crater.

(i) Elastic

Allen[30] has shown that the stresses produced by an explosive load at the surface of a semi-infinite plate have the same magnitude as that predicted by the elastic theory if the same charge was detonated in a small cavity at the center of an infinite sphere. We expect this agreement for a high velocity impact, since the phenomenon is similar to an explosion, i.e. high pressure of short duration.

In the present work, the results and theory give insufficient information to base any definite conclusions. Some of the limitations are obvious; for example, the increase in the radius of the cavity is assumed to be less than $Y/2E$ times the original radius, which is far too small. Hence, we have to take various values of a_o for different combination of pressure and its time of application. The imcompressible flow assumption implies an infinite rate of straining; in order to allow for this, a different value of Y will have to be assured for various impact velocities.

In the plot of the radius of the plastic zone against the velocity, fig. 5, the measured values fit theoretical points for values of $a_o Y_s / Y$ from slightly less than 1/100 at 3,920 ft/sec impact velocity, to slightly over 1/200 for 6,590 ft/sec impact velocity.

(ii) Elastic-Plastic

The elastic-plastic theory plot, fig. 6, indicates that the dynamic yield corresponding to impact velocities of 3,920 ft/sec and 6,590 ft/sec should be approximately 2.2. Y_s and 3.7 Y_s respectively. We note that above 5,300 ft/sec impact velocity the measured radius of the plastic zone closely follows the theoretical prediction, assuming a dynamic yield of 3.7 Y_s.

Taylor[21] has measured values for the yield stress in mild steel at high rates of strain. He found for a rate of straining of 10,000 in/in/sec that the dynamic yield was three times the static. The reasons for the increase in yield may be explained by consideration of the anchored dislocations just beyond the perimeter of the yielded region. These form obstacles to the passage of released dislocations from the region. The propogation of the yielding failure must involve the release of these anchored dislocations. If this is to happen quickly the stress on these dislocations must be high. Furthermore, Barrett[34] has pointed out that there is a greater increase in resistance in the soft metals than in the hard ones. The author has been unable to find any published work which relates to the dynamic yielding of 70:30 brass.

It can easily be shown that the von Mises and Tresca yield criterion will give the maximum shear stress as 0.58 Y and 0.50 Y respectively. Hence in the regions of very high pressure ($\sigma >> Y$), if we neglect shear, the error involved in calculating the stresses should not be high. However, this could lead to error in calculating the elastic-plastic boundary. For example, the von Mises yield condition in the axial symmetrical distribution of stress contains the term $6\tau^2_{Rz}$

i.e.

$$(\sigma_R - \sigma_\theta)^2 + (\sigma_\theta - \sigma_z)^2 + (\sigma_z - \sigma_R)^2 + 6\tau^2_{Rz} = 2Y^2$$

Now, Cook[2] has pointed out that when a single particle of nearly spherical shape strikes a target at high velocity, then the target undergoes plastic spherical deformation. (The exception is at the surface of the target where an elevated lip in always observed owing to some back flow caused by relief of pressure at the surface.) In this case, we expect the spherical assumption to be a good approximation, except at the surface.

5.4 Suggestions for Future Work

During the course of the present work, the author came upon several interesting problems where the present knowledge is either superficial or non-existent. Some of these are listed below under two headings (i) theoretical, and (ii) experimental.

(i) Theoretical.

(a) The calculation of the boundary of the plastic zone at higher velocity of impact, where compressibility would have to be taken into account.

(b) The calculation of the boundary of the plastic zone due to high velocity impact for a semi-infinite block target, assuming the target material to be incompressible; also for the compressible material.

(c) Theory for the dynamic yield at high rates of strain.

(ii) Experimental.

(a) Since more in known about the dynamical yield stress in steel a check could be made of the present theory using mild steel targets. This would check the theories (i a) and (i b). Details of the experimental technique may be found in Chapter 3.

(b) Estimate the impact pressure and its duration.

(c) Obtain the dynamic yield for several materials.

The solutions of these problems would add greatly to our understanding of the phenomenon of high velocity impact.

APPENDIX A

We are concerned with singular surfaces. (Weak type discontinuity, in that only discontinuities in the derivatives of the functions occur). which may occur to the von Mises and Prandtl-Reuss equations of plasticity. These equations are

$$\frac{\partial \rho}{\partial t} + \rho v_{\alpha,\alpha} = 0 \qquad \text{(Equ. of continuity)}$$

$$\sigma_{\alpha\beta,\beta} = \rho \frac{d v_\alpha}{dt} \qquad \text{(Equ. of motion)}$$

$$v_{\alpha,\alpha} = 0 \qquad \text{(Equation of incompressibility)}$$

$$\sigma^*_{\alpha\beta}\,\sigma^*_{\alpha\beta} = K \qquad \text{(quadratic yield condition)}$$

where the $\sigma^*_{\alpha\beta}$ are the components of the deviator stress tensor σ ,

$$d\varepsilon_{ij} = \sigma^*_{ij}\, d\lambda \qquad \text{(von Mises)}$$

or

$$\left.\begin{aligned} d\varepsilon^*_{ij} &= \sigma^*_{ij}\, d\lambda + \frac{d\sigma^*_{ij}}{2G} \\ d\varepsilon_{ii} &= \frac{1-2\nu}{E}\, d\sigma_{ii} \end{aligned}\right\} \text{(Prandtl-Reuss)}$$

Let $S(t)$ be the surface given by $f(x^i, t) = 0$ in a region $R(t)$ and that $f^{,i} f_{,i} > 0$, then

$$\nu_i = f_{,i} \Big/ \sqrt{f^{,i} f_{,j}}$$

is a unit vector normal to $S(t)$ and.

$$\theta = -\frac{\partial f}{\partial t} \Big/ \sqrt{f^{,j} f_{,j}}$$

is the displacement speed, i.e. the normal component of velocity, of $S(t)$. If $R(t)$ is occupied by a continuous medium moving with a velocity v^i which is continuous on $S(t)$ then $\theta - v^i \nu_i$ represents the normal component of velocity of $S(t)$ relative to the material particles instantaneously comprising it. If on this wave surface we assume $S(t)$ to be singular of order one., we take the density ρ the velocity components v_α and the stress components $\sigma_{\alpha\beta}$ continuous across $S(t)$ while at least one of their first partial derivatives with respect to space coordinates, is discontinuous at points of $S(t)$. Denoting by the bracket $[\ ]$ the difference in the values of a quantity on the two sides of $S(t)$ in the usual manner, it can be shown that for a singular surface $S(t)$ of order one, we shall have the relations,

$$[\sigma_{ij,k}] = \alpha_{ij} \nu_k ; \qquad \left[\frac{\partial \sigma_{ij}}{\partial t}\right] = -\alpha_{ij} \theta$$

$$[v_{i,k}] = \beta_i \nu_k ; \qquad \left[\frac{\partial v_i}{\partial t}\right] = -\beta_i \theta$$

$$[\rho, k] = \gamma \nu_k \quad ; \quad \left[\frac{\partial \rho}{\partial t}\right] = -\gamma\theta$$

where α_{ij} , β_i , and γ are quantities defined over $S(t)$, the ν_k are the components of the unit normal vector to the surface and θ denotes the velocity of the surface relative to the coordinate system in the direction specified by the vector .

BIBLIOGRAPHY

1. Rinehart, J. S. and Pearson, J., Behavior of Metals under Impulsive Loads, American Society for Metals, Cleveland, 1954.

2. Cook, M. A., Mechanism of Cratering in Ultra-High Velocity Impact, Explosives Research Group, University Of Utah, 1957.

3. Pack, D. C. and Evans, W. M., Penetration by High-Velocity (Munroe) Jets, Proceedings of the Physical Society, London, Vol. B 64, 1951.

4. Birkhoff, G., MacDougall, D. P., Pugh, E. M. and Taylor, G. T., Explosives with Lined Cavities, Journal of Applied Physics, Vol. 19, No. 6, June, 1948.

5. Engel, O. G., Journal of Research of the National Bureau of Standards, Vol. 62, No. 6, June, 1959.

6. Van Valkenburg, M. E., Clay, W. G. and Huth, J. H., Impact Phenomena at High Speeds, Journal of Applied Physics, Vol. 27, No. 10, 1956.

7. Partridge, W. S. and Clay, W. G., Studies of High Velocity Impact in Wall, Journal of Applied Physics, Vol. 29, No. 6, 1958.

8. Wessman, H. E. and Rose, W. A., Aerial Bombardment Protection, J. Wiley and Sons, Inc., New York, 1942.

9. Helie, F., Traite de Balistique Experimentale, Dumaine, Paris, 1884.

10. Kolsky, H., Stress Waves in Solid, Clarendon Press, 1953.

11. Davies, R. M., Stress Waves in Solids. Surveys in Mechanics, edited by Batchelor, G. K. and Davies, R. M., Cambridge University Press, 1956.

12. Abramson, H. N., Plass, H. J., and Ripperger, E. A., Stress Wave Propogation in Rods and Beams, Advances in Applied Mechanics, Vol. 5, 1958.

13. Kolsky, H., Propogation of Stress Waves in Viscoelastic Solids, Applied Mechanics Review, Sept., 1958.

14. Taylor, G. I., The Plastic Wave in a Wire Extended by an Impact Load, Taylor, G. I. Scientific Papers, Vol. 1, Cambridge University Press.

15 Von Karman, T., and Duwez, P., The Propogation of Plastic Deformations in Solids, Journal of Applied Physics, Vol. 21, 987, 1950.

16. Rakmatoolin, K. A., Propogation of Waves of Unloading, Translation No. 2, Brown University, Rhode Island.

17. Wood, D. S., On Longitudinal Plane Waves of Elastic-Plastic Strain in Solids, Journal of Applied Mechanics, Vol. 19, 521, 1952.

18. Craggs, J. W., The Propogation of Infinitesimal Plane Waves in Elastic-Plastic Materials, Journal of the Mechanics and Physics of Solids, Vol. 5, No. 2, 1957.

19. Thomas, T. Y., On the Propogation of Weak Discontinuities in Perfectly Plastic Solids, Journal of Mathematics and Mechanics, Vol. 6, No. 1, 1957.

20. Berg, C. A., Jr., Propogation of Stress Waves in an Elastic-Plastic Work-Hardening Material, S. M. Thesis, Department of Mechanical Engineering, Massachusetts Institute of Technology, 1958.

21. Taylor, G. I., Testing of Materials at High Rates of Loading, Taylor, G. I. Scientific Papers, Vol. 1, Cambridge University Press.

22. Campbell, J. D., The Yield of Mild Steel Under Impact Loading, Journal of Mechanics and Physics of Solids, Vol. 34, 1952.

23. Malvern, L. E., The Propogation of Longitudinal Waves of Plastic Deformation in a Bar of Material Exhibiting a Strain-Rate Effect, Journal of Applied Mechanics, Vol. 18, P. 203, 1951.

24. Bridgman, The Compressibility of Thirty Metals, Proceedings of the American Academy of Arts and Sciences, Vol. 58, No. 5, P. 166, 1923.

25. Walsh, J. M. and Christian, R. H., Equation of State of Metals from Shock Wave Measurements, Physics Review, Vol. 97, No. 6, P. 1544, 1955.

26. Walsh, J. M., Rice, M. H., McQueen, R. G., and Yarger, F. L., Shock-Wave Compressions of Twenty-Seven Metals, Equations of State of Metals, Physics Review, Vol. 108, No. 2, October, 1957.

27. Katz, S., Hugoniot Equation of State of Aluminum and Steel from Oblique Shock Measurements, Journal of Applied Physics, Vol. 30, No. 4, April, 1959.

28. Slater, J. C., Introduction to Chemical Physics, Chapter XIII, McGraw-Hill Book Company, New York, 1939.

29. Kumar, Sudhir, Scabbing in Bars and Plates-Further Studies, Technical Reports of O O R Project No. TB 2-0001 (1253), Pennsylvania State University, Report 13, March 1, 1958.

30. Allen, W. A., Free Surface Motion Induced by Shock Waves in Steel, Journal of Applied Physics, Vol. 24, No. 9, 1953.

31 Herrmann, W. and Leech, J., Analysis of Deformation of Various Configurations, Document 201, Aeroelastic and Structures Research Laboratory, Massachusetts Institute of Technology, September, 1959.

32. Simmons, J. A., Hauser, F., Dorn, J. E., Mathematical Theories of Plastic Deformation Under Impulsive Loading. University of California, Berkeley Report, Series No. 133, Issue No. 1, April, 1959.

33. Cottrell, A. H., Dislocations and Plastic Flow in Crystals. Oxford University Press, 1956.

34. Barrett, C. S., Structure of Metals, McGraw-Hill Book Company, 1952.

35. Eubanks, R. A., Muster, D., Volterra, E., An Investigation on the Dynamic Properties of Plastics and Rubber-like Materials, Proceedings of the Second U.S. Congress of Applied Mechanics, American Society of Mechanical Engineers, P. 193, New York, 1954.

36. Lee, E. H. and Kanter, T., Journal of Applied Physics, Vol. 24, P 1115, 1953.

37. Hillier, K. W., Proceedings of the Physical Society B, Vol. 62, P. 701, 1949.

38. Howarth, L., Editor, Modern Developments in Fluid Dynamics. High Speed Flow. Vol. 1, Oxford University Press, 1953.

39. Hill, R., The Mathematical Theory of Plasticity. Oxford University Press, 1956.

40. Prager, W. and Hodge, P. G., Jr., Theory of Perfectly Plastic Solids, John Wiley and Sons, 1951.

41. Love, A. E. H., The Mathematical Theory of Elasticity Oxford University Press, 1952.

42. Green, A. E. and Zerna, W., Theoretical Elasticity, Oxford University Press, 1954.

43. Hunter, S. C., A Study of High Speed Spherical Flow in Incompressible Metals, A.R.D.E. Report (Mx), October, 1958.

44. Samuels, L. E. and Mulhearn, T. O., An experimental Investigation of the Deformed Zone Associated with Indentation Hardness Impressions, Journal of the Mechanics and Physics of Solids, Vol. 5, P. 125 to 134, 1957.

45. Mulhearn, T. O., The Deformation of Metals by Vickers-Type Pyramidal Indenters, Journal of the Mchanics and and Physics of Solids, Vol. 7, No. 2, 1959.

46. Metals Handbook, American Society for Metals, 1948 Edition.

47. Avery, H. S., Homerberg, V. O., Cook, E, Metallographic Identification of Ferro-Magnetic Phases, Metals and Alloys, Vol. 10, 1939.

48. Wilson, D. V.
Journal of the Iron and Steel Institute, Vol. 176, 28, 1954.

49. Samuel, J.,
Journal of the Institute of Metals, Vol. 81, 471, 1952.

50. Samuel, J.

Journal of the Institute of Metals, Vol. 83, 359, 1954.

51. Ericksen, J. L., Singular Surfaces in Plasticity, Journal of Mathematics and Physics, Vol. 34, 1955.

52. Hadamard, J., Lecons sur la Propogation des Ordes et les Equations de l' Hydrodynamique, Hermann, A., Paris, 1903.